A strontium and neodymium isotopic study of Apollo 17 high-Ti mare basalts: Resolution of ages, evolution of magmas, and origins of source heterogeneities

JAMES B. PACES,[1,]* SHUN'ICHI NAKAI,[2] CLIVE R. NEAL,[1] LAWRENCE A. TAYLOR,[1] ALEX N. HALLIDAY,[2] and D-C. LEE[2]

[1] Department of Geological Sciences, University of Tennessee, Knoxville, TN 37996-1410, USA
[2] Department of Geological Sciences, University of Michigan, Ann Arbor, MI 48109-1063, USA

Abstract—A combined Sr and Nd isotopic study of 15 Apollo 17 high-Ti mare basalts was undertaken to investigate geochronological and compositional differences between previously identified magma types (A, B1, B2, and C). Whole-rock and mineral separates for one of the least-evolved Type B1 basalts, 70139, yield Sm-Nd and Rb-Sr isochron ages of 3.71 ± 0.12 Ga and 3.65 ± 0.13 Ga, respectively. A more-evolved, Type A basalt, 71539, exhibits a slightly older Sm-Nd isochron age of 3.75 ± 0.07 Ga and a Rb-Sr isochron age of 3.67 ± 0.10 Ga. Although these two ages are non-resolvable by themselves, compilation of all available geochronological data allows resolution of Type A and B1/B2 ages at high levels of confidence (>99%). The most reliably dated samples, classified according to their geochemical type, yield weighted average ages of 3.75 ± 0.02 Ga for Type A (N = 4) and 3.69 ± 0.02 Ga for Type B1/B2 (N = 3) basalts. Insufficient geochronological data are available to place the rare, Type C basalts within this stratigraphy. We propose that age differences correlate with geochemical magma type, and that early magmatism was dominated by eruption of Type A basalts while later activity was dominated by effusion of Type B1 and B2 basalts.

Whole-rock isotopic data yield distinct differences in initial Sr and Nd isotopic compositions between Types A, B1, B2, and C basalts. Types A, B1, and C exhibit restricted intra-group compositional variations and lie along well-defined whole-rock isochrons. These data are consistent with petrogenetic models involving closed-system fractionation of observed microphenocrysts from chemically and isotopically distinct parental magmas. In contrast, a wide range of Type B2 initial isotopic compositions indicates mixing of several distinct components during magma evolution.

The Sm-Nd whole-rock isochron age for Type A, B1, and C basalts of 3.79 ± 0.15 Ga is within error of Apollo 17 eruptive activity. However, the very well-defined Sr whole-rock isochron age of 4.02 ± 0.05 Ga is 270 to 330 Ma older than eruptive ages. Isotopic and petrological arguments indicate that extensive Rb/Sr fractionation did not occur at the time of melt generation. Therefore, the 4.0 Ga Sr whole-rock isochron age records a significant event at which time geochemical heterogeneities were established within the originally homogeneous basalt source regions. Types A and C sources were enriched in Rb/Sr, with little or no concurrent modification of $^{87}Sr/^{86}Sr$, Sm/Nd, or $^{143}Nd/^{144}Nd$. Infiltration of similar-aged KREEP magmas into mantle cumulate sources cannot explain both Sr and Nd isotopic data. Instead, we suggest a metasomatic origin in which Rb, transported as a chloride complex in halogen-rich fluids, was preferentially mobilized relative to Sr and the REEs.

INTRODUCTION

MAJOR-ELEMENT, TRACE-ELEMENT, AND isotopic studies of a wide variety of lunar mare basalts have led to the popularity of petrogenetic models requiring remelting of cumulates that formed during crystallization of a global magmasphere. Much of the first-order compositional variation among mare basalt groups can be attributed to gross, modal differences within cumulate layers constituting the mantle source regions. However, the more-limited compositional variations observed *within* an individual suite of basalts are often attributed to magmatic processes such as varied degrees of partial melting and closed- or open-system magmatic differentiation. These processes obscure the unambiguous identification of different primary melts which may, in turn, be related to small-scale heterogeneities within a particular mare basalt source region. In addition to the problem of resolving the scale of chemical

variability within individual source regions, stratigraphic resolution within a single suite of lavas is severely limited by the difficulties in lowering uncertainties associated with mare basalt age determinations to below about 80 Ma.

A large suite of Apollo 17 high-Ti mare basalts analyzed to date show overall compositional similarities; however, detailed studies reveal subtle patterns of systematic differences. Three distinct geochemical magma types have been identified as Types A, B, and C high-Ti basalts (WARNER et al., 1975, 1979; RHODES et al., 1976; NEAL et al., 1990a). Using an expanding geochemical data base, NEAL et al. (1990a) have further divided Type B basalts into B1 and B2 compositional types on the basis of trace-element ratios. An additional variant of high-Ti basalt, termed Type D and represented by a single sample (70091,2161), has REE abundances and patterns similar to Type B1 basalts, but distinct MgO, Cr_2O_3, and TiO_2 contents and warrants a distinct lineage (RYDER, 1990). Previous studies have underscored the importance of near-surface fractionation of olivine, spinel, and Ti oxides during petrogenesis (LONGI et al., 1974; GREEN et al., 1975;

---

* *Present address:* Branch of Isotope Geology, US Geological Survey, Mailstop 963, Denver Federal Center, Denver, CO 80225, USA.

WARNER et al., 1975, 1979; PAPIKE et al., 1976; RHODES et al., 1976; NEAL et al., 1990a). Although overall major-element similarities between the three basalt groups suggest closely related source compositions, trace-element arguments require separate parent magmas derived from distinct source areas for each compositional type (SHIH et al., 1975; RHODES et al., 1976; WARNER et al., 1979; NEAL et al., 1990a). In addition, WARNER et al. (1979) argued that varied degrees of partial melting were also required to explain La/Sm variations in Type B basalts (Fig. 1), whereas these same chemical trends have been attributed to assimilation of KREEP (NEAL et al., 1989). While radiogenic isotope geochemistry should have the potential to discriminate among these various petrogenetic models, earlier Sr isotopic work of NYQUIST et al. (1974, 1975, 1976) did not allow resolution of either ages or initial $^{87}Sr/^{86}Sr$ ratios between Types A and B mare basalts, though ages and Sr isotopic compositions of Rb-rich, Type C basalts were shown to be distinct (NYQUIST et al., 1976). The lack of isotopic resolution was due, in part, to the restricted compositional range of high-Ti basalts that had been identified during the mid-1970s (Fig. 1). Subsequent geochemical studies have greatly increased both major- and trace-element compositional ranges of each of the geochemical types of Apollo 17 high-Ti basalts. The expanded geochemical database currently available requires re-examination of isotopic variations within the Apollo 17 mare basalt suite. In addition, only a small number of Nd isotopic analyses of Apollo 17 high-Ti basalts are presently available, and in only a few cases have both Nd and Sr isotopic compositions been acquired from the same sample. Previous Nd studies that included Apollo 17 basalts (LUGMAIR et al., 1975; NYQUIST et al., 1979; UNRUH et al., 1984) focused on Moon-wide, mare basalt comparisons and have not concentrated on compositional differences within the Apollo 17 suite.

In this study, we present high-precision Rb-Sr and Sm-Nd isotopic data for a set of Apollo 17 samples chosen to span the range of each of the previously defined geochemical types. Our objectives are to ascertain whether or not resolvable age and compositional relationships exist among the different basalt types, and to determine whether observed differences are related to post-melt magma modifications or to heterogeneities within distinct Apollo 17 high-Ti basalt sources. In order to address these questions, we present two new Rb-Sr and Sm-Nd internal isochron ages on basalts of unambiguous geochemical type. These data, combined with previously published ages, suggest that Apollo 17 volcanism was initially dominated by eruption of Type A basalts which gave way to later predominance of Type B basalts. We also present 15 new whole-rock Sr and Nd isotopic analyses which are used to test petrogenetic models. Subtle isotopic compositional variations observed between Types A, B1, and C magmas are used to provide further constraints on the composition and geochemical evolution of the Apollo 17 high-Ti mantle source regions.

SAMPLING AND ANALYTICAL PROCEDURES

Basalts from each of the three geochemical groups exhibit a variety of textures which have been described in previous petrographic studies (PAPIKE et al., 1974; BROWN et al., 1975; DYMEK et al., 1975; WARNER et al., 1975; NEAL et al., 1990a). The two predominant textural types of basalt analyzed in this study are fine-grained (<1 mm) olivine microporphyritic, and relatively coarse-grained (>2 mm) plagioclase-poikilitic varieties. Mineralogy is dominated by pinkish-brown pyroxene (titan-augite followed by pigeonite), plagioclase, and ilmenite.

Samples consisted of basalt fragments, small chips, or homogeneous fines weighing 150–750 mg which were coarsely crushed in a boron carbide mortar under a laminar flow of better than class 10 clean-room quality air. Representative whole-rock samples were obtained by quarter-splitting an approximately 100 mg aliquot which was further powdered. Two samples, 70139,6 and 71539,6, were chosen for mineral isochron dating. 70139 is a Type B1 basalt with a relatively coarse-grained, plagioclase-poikilitic texture. A 445 mg fragment was repeatedly crushed and sieved to coarse (100–250 μm) and fine (50–100 μm) size fractions. Washed particles were separated into four magnetic fractions, and further hand-picking of coarse fractions resulted in pure ilmenite (Ilm) and pyroxene (Px) separates. Coarse magnetic (Mag; pyroxene + ilmenite) and non-magnetic (NMag; plagioclase + pyroxene) composite fragments, as well as the fine non-magnetic (F Plg; >95% plagioclase) fraction were also analyzed. 71539 is a Type A basalt exhibiting a fine-grained, olivine microporphyritic texture, and weighing 759 mg. After removal of the whole-rock aliquot, the remaining material was treated similarly to 70139. The finer grain-size of 71539 required crushing of all material to 50–100 μm size fraction. Similar magnetic separates were treated with heavy liquids followed by hand-picking to yield two plagioclase (Plg1, Plg2), one pyroxene (Px1), and two ilmenite (Ilm1, Ilm2) fractions, as well as magnetic (Mag1) and non-magnetic (NMag1) mixtures. All fractions were picked under spectrographic-grade methanol and were cleaned by cold, ultrasonic washes in methanol, distilled acetone, and deionized water. Mineral separates weighed between 7 and 58 mg, and each separate was total-spiked before digestion with known ^{87}Rb, ^{84}Sr, ^{149}Sm, and ^{150}Nd tracers. Whole-rock samples weighing between 37 and 68 mg were first dissolved, after which solutions were split into unspiked and spiked aliquots. Two-stage cation separations followed standard techniques described elsewhere (HALLIDAY et al., 1989). Average total-process blanks for chemical procedures were 20 pg Rb, 70 pg Sr, 17 pg Sm, and 70 pg Nd.

Isotopic data were obtained on VG Sector multicollector thermal ionization mass spectrometers. Strontium was loaded, along with Ta_2O_5 powder, onto single Re filaments while Rb was loaded onto triple Ta filament assemblies. Samarium and neodymium were loaded onto triple Ta-Re-Ta filament assemblies, and both were measured as metal ions. Isotope dilution measurements were made using static simultaneous multicollection of 40–80 ratios. Strontium and neo-
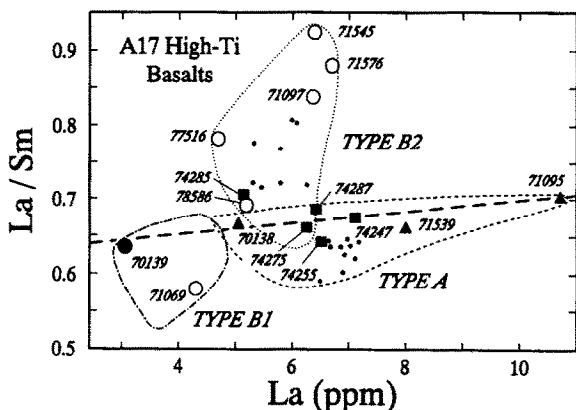

FIG. 1. La/Sm versus La for samples analyzed for Sr and Nd isotopes in this study (data from RHODES et al., 1976; WARNER et al., 1975, 1979; MURALI et al., 1977; NEAL et al., 1990a). Solid triangles = Type A basalt; solid circle = Type B1 basalt; open circles = Type B2 basalt; and solid squares = Type C basalt. Small dots represent basalts analyzed for Rb-Sr isotopes in the mid-1970s (NYQUIST et al., 1974, 1975, 1976). Bold, dashed line indicates sub-horizontal trend of La/Sm in Types A, B1, and C basalts. Field boundaries from NEAL et al. (1990a).

TABLE 1: Rb-Sr and Sm-Nd analytical results for whole rocks and mineral separates used for internal isochrons.

Sample	Wt.(mg)	Rb (ppm)	Sr (ppm)	$^{87}Rb/^{86}Sr^a$	$^{87}Sr/^{86}Sr^b$	Sm (ppm)	Nd (ppm)	$^{147}Sm/^{144}Nd^a$	$^{143}Nd/^{144}Nd^b$
70139,6 Type B1									
WR1	66.90	0.281	146	0.005515±55	0.699511±14	5.30	12.3	0.26021±52	0.514547±11
WR2	65.28	0.282	146	0.005543±55	0.699518±17	5.38	12.4	0.26234±52	0.514605±15
F Plg	8.80	0.0886	514	0.004956±20	0.699244±27				
Ilm	16.83	0.313	23.1	0.03903±39	0.701312±31	3.49	8.54	0.24726±49	0.514230±23
Px	37.42	0.143	30.2	0.01364±14	0.699922±32	4.85	9.72	0.3020±15	0.515571±29
Mag^c	46.23	0.478	87.9	0.01564±16	0.700013±28	9.17	21.5	0.2574±26	0.514457±25
NMag^c	28.60	0.0882	270	0.000939±18	0.699297±25	1.82	3.89	0.28250±56	0.515098±26
71539,6 Type A									
WR	36.93	0.787	229	0.009893+98	0.699776±14	13.4	32.5	0.25018±50	0.514306±11
Plg1	30.54	0.260	623	0.001199±11	0.699336±22	2.08	5.70	0.2204±22	0.513565±19
Plg2	12.13	0.594	536	0.003192±31	0.699382±20	5.91	15.2	0.2352±24	0.513899±20
NMag1^c	19.45	0.188	253	0.002139±21	0.699360±21		9.20		0.513868±20
Px1	43.86	0.121	58.7	0.005917±59	0.699564±22	5.12	9.22	0.3362±17	0.516428±18
Mag1^c	57.70	0.573	103	0.01602±32	0.700119±20				0.514780±16
Ilm1	8.89	1.23	104	0.03395±34	0.701188±20	18.4	38.3	0.2900±14	0.515283±22
Ilm2	6.87	0.642	128	0.01444±14	0.700033±20		22.4		0.514350±19

^{a} Uncertainties (corresponding to last decimal places) reported for parent/daughter ratios reflect the magnitude of the blank correction, mass spectrometer precision and corrections for the quality of spiking.

^{b} Normalized to $^{86}Sr/^{88}Sr=0.1194$ and $^{146}Nd/^{144}Nd=0.7219$. Quoted errors include 2 sigma run precision for whole rock analyses plus an additional uncertainty of 0.00001 (2 sigma) reflecting corrections for fractionation and spike contributions in total-spiked mineral separates. Nd was measured as the metal ion.

^{c} Non-pure mineral separates consisting of predominantly "nonmagnetic" plagioclase and pyroxene in NMag and "magnetic" pyroxene and ilmenite in Mag.

dymium isotopic compositions on unspiked aliquots were measured using multidynamic analysis of about 200 ratios with resulting precisions of 0.001-0.003% (2 sigma). All Sr and Nd analyses are normalized to $^{86}Sr/^{88}Sr = 0.1194$ and $^{146}Nd/^{144}Nd = 0.7219$, respectively. Fifteen analyses of NBS987 Sr and La Jolla Nd standards analyzed over the same time period yielded weighted averages of $^{87}Sr/^{86}Sr = 0.710251 \pm 0.000009$ and $^{143}Nd/^{144}Nd = 0.511866 \pm 0.000005$. The effects of neutron bombardment lowering Sm concentrations by depletion of ^{149}Sm have been ignored in this study. NYQUIST et al. (1979) estimated a 0.2% decrease in the Sm/Nd ratio on 75075 from the Sm isotopic measurements of LUGMAIR et al. (1975). Although varying lengths of exposure on the lunar surface for the different samples may cause some scatter, the concordance of data for all Type A, B1, and C samples on the same isochron indicates that exposure effects are not detrimental to the Sm-Nd dating technique for the present suite of rocks. Age calculations use decay constants of 6.54 × 10^{-12} yr^{-1} for ^{147}Sm and 1.42 × 10^{-11} yr^{-1} for ^{87}Rb (STEIGER and JÄGER, 1977). Although the 1.42 × 10^{-11} yr^{-1} constant has become internationally accepted for all terrestrial and many extraterrestrial studies, combined isotopic studies on ancient lunar and some meteoritic materials suggest that the older Rb-Sr ages obtained using a 1.39 × 10^{-11} yr^{-1} decay constant for ^{87}Rb are, in some instances, in better concordance with other isotopic systems (MINSTER et al., 1982; NYQUIST et al., 1986; SHIH et al., 1986). However, this issue is complicated by the possibility of post-magmatic mobility of Rb and Sr due to impact heating associated with sample excavation (see geochronology section). Until these factors are better understood, we prefer to use the standardized 1.42 × 10^{-11} yr^{-1} value for the ^{87}Rb decay constant. Two additional samples of extraterrestrial materials have been analyzed over the same time period: a coarse-grained Apollo 15 olivine tholeiite, 15555,817, and a split of the Smithsonian Allende carbonaceous chondrite meteorite standard, USNM 3529. Variations in Rb, Sr, Sm, and Nd concentrations and present-day isotopic com-

positions of replicate analyses indicate that both samples contain mineralogical inhomogeneities on the scale of the 35 to 45 mg powders digested for analysis. However, calculated initial ratios between replicates are nearly identical, and show initial ratios and associated errors which are within error of previously published results.

GEOCHRONOLOGICAL INVESTIGATION

Internal Isochron Results

Results of isotopic analyses for 70139 and 71539 whole rocks and mineral separates are listed in Table 1. In both cases, Rb-Sr and Sm-Nd isochron plots yield linear arrays of data (Figs. 2 and 3). The small range of parent/daughter ratios present in the mineral phases limits the uncertainty of the calculated ages to no better than 70 to 130 Ma. For both rocks, Rb-Sr ages are 60 to 80 Ma younger than Sm-Nd ages. Although Rb-Sr and Sm-Nd ages for both rocks are nearly identical when the 1.39 × 10^{-11} yr^{-1} ^{87}Rb decay constant is used, lower Rb-Sr ages relative to Sm-Nd ages are commonly observed in other studies, even when "older" Rb-Sr ages are calculated using the 1.39 × 10^{-11} yr^{-1} decay constant (e.g., NYQUIST et al., 1981; SHIH et al., 1986). In addition, several of the individual mineral fractions described below show abnormal deviations of Rb-Sr isotopic data from the best-fit regressions and may imply that the Rb-Sr system was more easily disturbed than Sm-Nd during excavation of these two rocks. Until the Rb decay constant is better determined, Sm-Nd ages are considered most representative of the actual
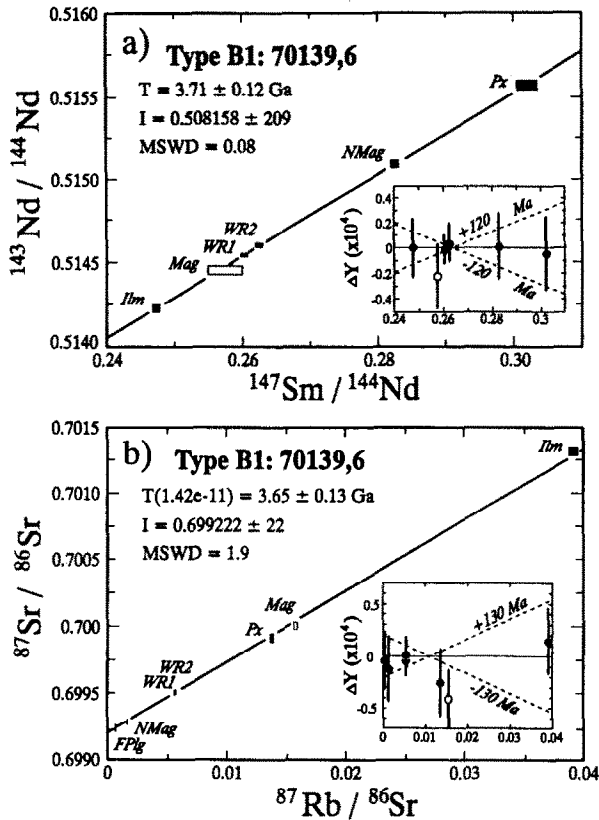
FIG. 2. (a) Sm-Nd and (b) Rb-Sr internal isochrons for 70139,6. Size of error boxes representing data points are drawn in proportion to uncertainties given in Table 1. Age and initial ratios were calculated using Model 1 York regression slope and intercept (YORK, 1969; LUDWIG, 1990). Strontium age is calculated with ^{87}Rb decay constant of 1.42×10^{-11} yr^{-1} ($T = 3.73$ Ga using λ^{87}Rb $= 1.39 \times 10^{-11}$ yr^{-1}). Data represented by the open symbols are not included in the isochron regression. All uncertainties quoted at the 95% confidence limit. Insets show the deviations of ^{143}Nd/^{144}Nd and ^{87}Sr/^{86}Sr from the regressed isochron in parts per 10,000 along with error limits both for individual data points (error bars), and for the regression line (dashed lines).

crystallization ages. All isochrons are calculated as Model 1 regressions (based on the original algorithm of YORK, 1969) using the program of LUDWIG (1990). Uncertainties are calculated using the maximum-likelihood algorithm of TITTERINGTON and HALLIDAY (1979) and, in all cases, are reported at the 95% confidence limit. Resulting ages for each rock are examined briefly below.

Type B1: 70139,6

Sm-Nd data for all fractions (four mineral separates and two whole-rock samples, Table 1) yield an age of 3.72 ± 0.12 Ga (Fig. 2a). The regression spans a very limited range of ^{147}Sm/^{144}Nd values with pyroxene-rich separates at the high ^{147}Sm/^{144}Nd end and ilmenite-rich separates at the low end. The pyroxene + ilmenite mixed fraction (*Mag*) contains REE abundances which are about twice as high as either the pure pyroxene or ilmenite fractions. We suspect that this fraction includes brownish mesostasis with high REE abundances, similar in appearance to the pinkish-brown pyroxene. This is consistent with Rb abundances which are also higher in

the *Mag* fraction than in any of the other fractions. Since the glassy portions of the rock are more likely affected by mild heating associated with post-crystallization impact and exposure processes, the presence of mesostasis in this fraction may increase the possibility of subsequent partial resetting. Regression of the data excluding the *Mag* fraction (i.e., *WR1*, *WR2*, *Px*, *NMag*, and *Ilm*) results in a nearly identical age of 3.71 ± 0.12 Ga with a very low MSWD of 0.08 (see Fig. 2). We consider this date to be the best Sm-Nd isochron age for 70139.

Rb-Sr data for all mineral fractions yield an age of 3.62 $\pm$ 0.15 Ga (Fig. 2b). The ^{87}Sr/^{86}Sr intercept value of 0.699222 $\pm$ 0.000022 is well defined due to the extremely low ^{87}Rb/ ^{86}Sr values in plagioclase separates. Regression of all data results in a MSWD of 2.84 which indicates a greater amount of scatter from the best-fit regression relative to the Sm-Nd isochron (inset, Fig. 2b). As noted earlier, the mixed pyroxene + ilmenite fraction, *Mag*, contains higher Rb and Sr concentrations than either of the two mineral phases analyzed alone. This fraction falls below the best-fit regression and is suspected of containing glassy mesostasis. If the *Mag* fraction is excluded from the regression, a slightly higher age of 3.65 $\pm$ 0.13 Ga is obtained with a slightly improved MSWD of 1.9. Although we cannot discount the possibility of analytical artifacts, we suspect that the observed scatter may be due to
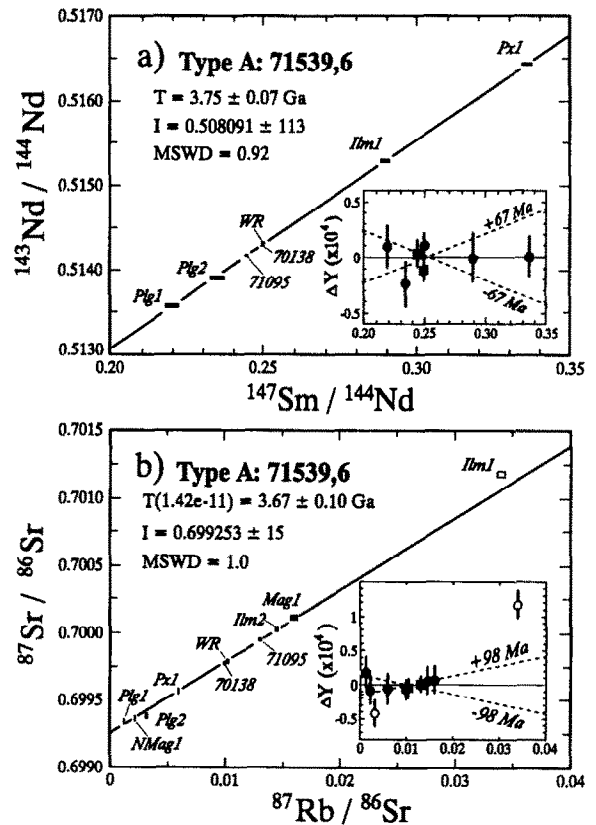

FIG. 3. (a) Sm-Nd and (b) Rb-Sr internal isochrons for 71539,6 (Sr isochron age = 3.75 Ga using λ^{87}Rb $= 1.39 \times 10^{-11}$ yr^{-1}). Details listed for Fig. 2 apply equally to Fig. 3 with the added comments: 70139 and 71095 are additional Type A whole-rock samples listed in Table 3 and have been included in the regression. See text for discussion.

mobility of Rb or Sr on a mineral-sized scale, particularly associated with glassy mesostasis adhering to the opaque fragments. However, Rb and Sr were probably not disrupted on the larger, whole-rock scale, where a substantially more-precise Rb-Sr isochron is obtained from samples which span a smaller Rb/Sr range. Although disturbances of the Rb-Sr system have not been evident in earlier work, the improved analytical precision attainable with the new generation of mass spectrometers may permit recognition of geological errors which were previously unresolved from analytical errors.

Type A: 71539,6

Regression of all Sm-Nd data (one whole-rock and four mineral fractions, Table 1) yields an age of 3.73 ± 0.07 Ga (Fig. 3a). The range in $^{147}Sm/^{144}Nd$ for mineral separates from 71539 is larger than that observed for 70139 and includes two analyses for plagioclase which display the lowest $^{147}Sm/^{144}Nd$ values. Unlike 70139, Sm and Nd abundances of the ilmenite fractions in 71539 are about two to four times higher than those in the pyroxene fraction. Rubidium concentration in at least one of the ilmenite fractions is also much higher than any of the other mineral separates. Although 71539 (Type A) is much more geochemically evolved than 70139 (Type B1), equilibrium partitioning of incompatible trace elements cannot explain the differences in ilmenite compositions. We suspect that the ilmenite in 71539 may be intergrown with minor amounts of mesostasis. Regardless of this possibility, the *Ilm1* fraction plots on the best-fit Sm-Nd regression line. Two additional Type A whole-rock analyses, 70138 and 71095 (data in Table 3), also plot on the 71539 mineral isochron (Fig. 3a) and are most likely related. The resulting regression yields a slightly older age of 3.75 ± 0.07 Ga with an MSWD of 0.92. This date, which includes a larger number of data points, is considered to represent the best Sm-Nd age for 71539.

Rb-Sr isotopic data for 71539 exhibit scatter in its linear array which cannot be attributed to analytical error. Regression of all data (one whole-rock and seven mineral analyses) yields an age of 3.83 ± 0.17 Ga (Fig. 3b). This Rb-Sr age is substantially older (80 Ma) than the Sm-Nd age; however, the large uncertainties associated with the Rb-Sr regression do not allow resolution of the two ages. Much of the excessive scatter in this regression (MSWD = 8.3) can be attributed to the ilmenite fraction, *Ilm1*, and the range in isotopic compositions of the plagioclase-rich fractions. As noted earlier, the ilmenite-rich fraction is suspected of containing Rb- and REE-enriched mesostasis in which more-volatile Rb abundances may be mobilized during impact heating. In addition to *Ilm1*, one of the plagioclase separates, *Plg2*, deviates from the best-fit line more than other samples. This fraction is a smaller and less-pure separate than *Plg1*, and has substantially higher Rb and REE contents than either of the other two plagioclase-rich fractions (*Plg1* and *NMag1*, Table 1). If this point, along with *Ilm1*, is excluded from regression, an age of 3.67 ± 0.11 Ga is obtained with I(Sr) = 0.699253 ± 0.000015. The MSWD of 1.0 for this regression is substantially reduced. The two additional Type A whole-rock analyses (71038 and 71095, Table 3) also fall on the 71539 internal isochron (Fig. 3b). Inclusion of these two additional

data points in the Sr regression analysis yields an age of 3.67 ± 0.10 Ga, which is the best estimate of the internal Rb-Sr isochron age for 71539. Although the aberrant behavior of *Ilm1* and *Plg2* separates may be caused by analytical artifacts, these same samples do not show excessive scatter on the Sm-Nd isochron plot. The consistent patterns of Rb-, Sr-, and REE-enrichments in both *Ilm1* and *Plg2* mineral fractions, combined with the well-defined Sm-Nd isochron, suggest a geological, rather than analytical, cause for excessive Rb-Sr scatter.

Summary of ages for 70139 and 71539

The best age estimates for the Type B1 basalt, 70139, and the Type A basalt, 71539, are 3.71 ± 0.12 Ga and 3.75 ± 0.07 Ga, respectively, based on the Sm-Nd internal isochrons. In both cases, the Sm-Nd isochron ages are preferred over Rb-Sr ages because of the slightly smaller uncertainties associated with Sm-Nd regressions, and because of the controversy surrounding the choice of the most appropriate ^{87}Rb decay constant. However, it should be noted that if an ^{87}Rb decay constant of 1.39×10^{-11} yr^{-1} is used, very good agreement exists between the two systems, providing further support of the Sm-Nd ages. One possible explanation for discordance between Sm-Nd and Rb-Sr ages using the 1.42×10^{-11} yr^{-1} decay constant is that the minerals within both basalts had their Rb-Sr, but not their Sm-Nd, systematics disturbed by a younger impact event. Although none of the Apollo 17 basalts show signs of extensive shock metamorphic recrystallization, the younger Rb-Sr internal isochron ages for both rocks, plus excessive Rb-Sr scatter observed for some mineral separates, suggest that Sr ages, by themselves, should be approached with caution.

Although the Type A basalt appears to be older than the Type B1 basalt, uncertainties associated with each individual age determination are larger than the apparent age difference of 40 Ma. These data alone leave questions of magmatic stratigraphy and duration of volcanism at the Apollo 17 unanswered. However, in spite of the inherent difficulty in determining high-precision isochron ages on basalts exhibiting such limited variation in Rb/Sr and Sm/Nd ratios, uncertainties can be significantly lowered by increasing the number of observations. Examination of the larger set of published age determinations on Apollo 17 high-Ti mare basalts is helpful towards this goal.

Ages of Apollo 17 Volcanism

Twenty-eight published Rb-Sr, Sm-Nd, or ^{40}Ar-^{39}Ar dates on fifteen different Apollo 17 mare basalts have been determined over a period from 1973 to the present study (Table 2, Fig. 4). Ages range from 3.64 to 3.84 Ga. In general, ages obtained on the same basalt by different techniques and/or by different laboratories agree within error limits of individual age determinations. For the purposes of consistency, all isochron regressions have been recalculated using the Model 1 Yorkfit routine of LUDWIG (1990), and Rb-Sr age determinations have been calculated using the 1.42×10^{-11} yr^{-1} ^{87}Rb decay constant. This results in younger Rb-Sr ages than previously reported due to the former use of the 1.39×10^{-11}

Table 2: Available geochronological data for Apollo 17 high-Ti mare basalts.

Sample	Type[a]	Age (Ma)[b]	Method	Reference	"Best-Age" Estimate (Ma)
70135	A	3670 ± 84	Sr	Nyquist et al., 1975	3770 ± 60[c]
		3770 ± 60	Nd	Nyquist et al., 1979	
70215	A	3790 ± 40	Ar	Kirsten and Horn, 1974	
70255	A	3840 ± 20	Ar	Schaeffer & Schaeffer, 1977	
71539	A	3670 ± 98	Sr	This study	3750 ± 67[c]
		3750 ± 67	Nd	This study	
75035	A	3720 ± 40	Ar	Turner and Cadogan, 1975	3723 ± 38[d]
		3750 ± 120	Sr	Murthy and Coscio, 1976	
75055	A	3760 ± 50	Ar	Turner et al., 1973	3761 ± 32[d]
		3770 ± 50	Ar	Kirsten et al. 1973	
		3780 ± 40	Ar	Huneke et al., 1973	
		3690 ± 70	Sr	Tera et al., 1974	
70035	B	3690 ± 70	Ar	Stettler et al., 1973	3688 ± 56[d]
		3670 ± 110	Sr	Nyquist et al., 1974	
		3730 ± 190	Sr	Evensen et al., 1973	
70017	B	3610 ± 190	Sr	Nyquist et al., 1975	
70139	B1	3650 ± 120	Sr	This study	3710 ± 120[c]
		3710 ± 120	Nd	This study	
71055	B	3560 ± 90	Sr	Tera et al., 1973	
75075	B	3690 ± 20	Ar	Horn et al., 1975	3694 ± 19[d]
		3700 ± 70	Nd	Lugmair et al., 1975	
		3760 ± 150	Sr	Nyquist et al., 1975	
		3780 ± 110	Sr	Murthy and Coscio, 1976	
74255	C	3630 ± 140	Sr	Murthy and Coscio, 1976	3722 ± 67[d]
		3750 ± 77	Sr	Nyquist et al., 1976	
74275	C	3730 ± 320	Sr	Nyquist et al., 1976	
75083	U	3700 ± 90	Ar	Huneke et al., 1973	
79155	U	3750 ± 40	Ar	Kirsten and Horn, 1974	

[a] 70139 is the only Type B sample with sufficient geochemical data to permit B1/B2 classification. Chemical type for 75083 and 79155 remains undefined due to lack data.

[b] All Sr and Nd isochron ages regressed using Ludwig (1990) with $\lambda^{87}Rb = 1.42 \times 10^{-11}$ yr^{-1}.

[c] Best estimate based on Nd internal isochron age.

[d] Best estimate based on weighted average age of multiple age determinations.

yr^{-1} decay constant and in slightly different uncertainties (usually higher) due to the more rigorous assessment of 95% confidence errors by the LUDWIG (1990) regression analysis. In three out of the four rocks possessing both Rb-Sr and Sm-Nd internal isochron dates, Rb-Sr age determinations are 60 to 100 Ma younger than the Sm-Nd ages, while, in the fourth rock, two Rb-Sr age determinations are 60 to 80 Ma older. In rocks with both Rb-Sr and ^{40}Ar-^{39}Ar data, Rb-Sr age determinations can be younger, older, or very similar to ^{40}Ar-^{39}Ar dates, which typically have much smaller reported uncertainties. In the only sample possessing Rb-Sr, Sm-Nd, and ^{40}Ar-^{39}Ar ages (75075), very good agreement exists between Sm-Nd and ^{40}Ar-^{39}Ar ages, and between the Rb-Sr ages determined by two separate labs; however, both Sr ages are older than (although within error of) the Sm-Nd and ^{40}Ar-^{39}Ar ages. This discrepancy is further exacerbated when the 1.39 × 10^{-11} yr^{-1} ^{87}Rb decay constant is used.

The existing geochronological data set underscores the need for further high-precision age determinations by multiple techniques on the same rock. However, current data is helpful in revealing general age relationships between the different geochemical basalt types. Where multiple-age determinations

are available for the same basalt, we have made "best-age" estimates (Table 2) based either on Sm-Nd ages, where only Sm-Nd and Rb-Sr ages have been determined, or on weighted averages of any combinations of the three different techniques. In addition, we have assigned a chemical classification to each dated rock where possible. This is greatly facilitated by the use of Rb and Sr concentrations determined by isotope dilution on whole rocks dated by the internal Rb-Sr isochron technique (Fig. 5). Although chemical classification of Apollo 17 mare basalts is based on a larger number of elemental characteristics (RHODES et al., 1976; WARNER et al., 1979; NEAL et al., 1990a), accurate Rb concentrations are particularly diagnostic of each geochemical group, showing progressive enrichment from Type B1/B2, to Type A and, finally, Type C basalts. Previously dated Type B basalts cannot be classified as Types B1 or B2 without additional REE data; however, we suspect that both magma types are represented in the present data set. Out of the 15 dated basalts, 6 are classified as Type A, 5 as Type B1/B2, and 2 as Type C (Fig. 4). Two remain undefined due to lack of geochemical data.

The weighted average age for all 28 dates from the 15 basalts is 3.72 Ga ± 0.04 Ga (external population error of 0.13 Ga).
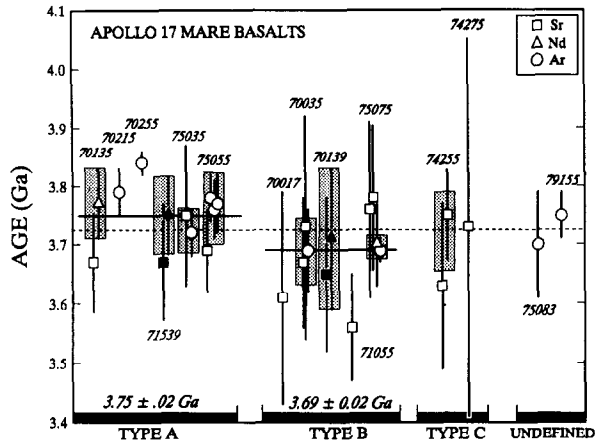
FIG. 4. Compilation of present (solid symbols) and published (open symbols) ages available for Apollo 17 high-Ti mare basalts (data and sources listed in Table 2). Symbol shape denotes the type of age determination: squares for Rb-Sr isochrons; triangles for Sm-Nd isochrons; and circles for ^{40}Ar-^{39}Ar techniques. Shaded boxes represent limits for "best-estimate" ages listed in Table 2. Dashed line represents the weighted average age of 3.72 ± 0.04 for all data. Basalts are also grouped by geochemical type and yield weighted average ages (solid horizontal lines) of 3.75 ± 0.02 Ga for Type A basalts and 3.69 ± 0.02 Ga for Type B basalts. See text for discussion.

If only the "best-age" estimates from samples with multiple age determinations are considered, a better-defined weighted average age of 3.72 ± 0.01 Ga is obtained. This age is interpreted to represent the current best estimate of the average age of Apollo 17 high-Ti mare basalt volcanism. However, Type A basalts show a noticeable tendency towards slightly older ages relative to Type B1/B2 basalts (Fig. 4). Averaged separately using only the "best-age" estimates, Type A basalts yield a weighted mean age of 3.75 ± 0.02 Ga while Type B1/B2 basalts yield a weighted mean age of 3.69 ± 0.02 Ga. The low uncertainties associated with these weighted averages allow the 60 Ma age difference between the two groups to be clearly resolved at the 95% confidence level. Further student-t testing of the seven Type A and B1/B2 "best-age" estimates (five degrees of freedom) indicates that the two populations are distinct at the 99% confidence level. Ages for Type C basalts are represented by three Rb-Sr dates from two rocks, and only one of these, 74255, is known with reasonable certainty. Ages of 3.72 ± 0.07 Ga for 74255 and 3.73 ± 0.32 Ga for 74275 (Table 2) are intermediate between average ages for Types A and B1/B2 volcanism. Previously reported ages for these rocks used the 1.39×10^{-11} yr^{-1} ^{87}Rb decay constant, resulting in ages up to 3.83 Ga (NYQUIST et al., 1976); however, no independent geochronometer has been applied to these samples. Additional dating using Sm-Nd and/ or ^{40}Ar-^{39}Ar chronometers is required before Type C basalts can be placed within the relative stratigraphy of Apollo 17 volcanism.

Presently available data suggest that duration of Apollo 17 high-Ti mare basalt volcanism lasted at least 50 Ma, but probably less than 200 Ma. We propose that age differences are correlatable to geochemical magma type, and that early magmatism was dominated by the eruption of Types A basalts while later activity was dominated by effusion of Type B1/

B2 basalts. The compositional transition may have occurred as two (or more) discrete pulses of magmatic activity separated by a significant hiatus, or activity may have taken place over a continuous, extracted episode with compositional changes occurring gradually throughout the stratigraphic interval. The inability to discriminate between B1 and B2 magmas provides an additional geochronological uncertainty given the complicated petrologic relationships between, as well as within, these two basalt groups. Further dating of well-analyzed samples may show that these two groups do not have a common age. However, present data are sufficient to indicate that, at least, Type B1 (and presumably B2 as well) basaltic activity was resolvably *younger* than that which produced most of the Type A basalts. The proposed chronology of *earlier* Types A magmas and *later* Type B1/B2 magmas is consistent with the relative abundances of heat-producing incompatible elements observed in the different lava types (RHODES et al., 1976; WARNER et al., 1979; NEAL et al., 1990a), particularly the radioactive alkali elements, K and Rb. Whole-rock isotopic data, presented in the next section, indicate that these compositional differences do not arise from fractionation processes alone and that these patterns were inherited from heterogeneous mantle sources.

WHOLE-ROCK ISOTOPIC DATA

Isotopic Compositions

Fifteen whole-rock samples were chosen to best represent the geochemical variability observed within each geochemical group (Fig. 1). Results of Sr and Nd isotopic analyses (Table 3) are comparable with previously reported data on Apollo 17 high-Ti basalt (NYQUIST et al., 1974, 1975, 1976, 1979; LUGMAIR et al., 1975; UNRUH et al., 1984). Initial isotopic compositions calculated at the estimated eruptive ages exhibit only a limited range of I(Sr) variation within Types A (0.699235 to 0.699240) and C (0.699274 to 0.699301) groups, but a much broader range of I(Sr) for Types B1 and B2 basalts (0.699140 to 0.699239). Types A, B1, and C basalts also show limited ϵ_{Nd} variation (+6.3 to +7.2) which is further reduced if all samples are calculated at the same age (+6.5 to +6.9 at $T = 3.72$ Ga). As with I(Sr), initial ϵ_{Nd} in Type B2 lavas exhibit a much wider range of values from as low as +2.7 up to +6.0. Given the good agreement of replicate analyses on 70139, along with the narrow range of initial Nd isotopic compositions in Types A, B1, and C basalts, the wide range of initial ϵ_{Nd} values observed in Type B2 samples (which were classified previously on the basis of their trace-element compositions; NEAL et al., 1990) is not considered to be an analytical artifact nor the result of preferential neutron bombardment on B2 samples alone. The wider ranges of initial Sr and Nd isotopic compositions observed in Type B2 basalts are interpreted to represent a fundamental difference between these and the Types A, B1, and C basalts. Model ages for all samples, based on the best estimated lunar initial Sr composition (T_{LUNI}; NYQUIST et al., 1974b) and chondrite uniform reservoir (T_{CHUR}; DEPAOLO and WASSERBURG, 1976), approximate or exceed the age of the Moon (Table 3), indicating multi-stage evolution of Rb-Sr and Sm-Nd within the basalt source regions.

TABLE 3: Whole rock Rb-Sr and Sm-Nd analytical results for Apollo 17 high-Ti mare basalts.

Sample	Chem. Type	Wt. (mg)	Rb (ppm)	Sr (ppm)	$^{87}Rb/^{86}Sr$	$^{87}Sr/^{86}Sr$	I(Sr)[a]	T_{LUNI} (Ga)[b]	Sm (ppm)	Nd (ppm)	$^{147}Sm/^{144}Nd$	$^{143}Nd/^{144}Nd$	I(Nd)[a]	$\varepsilon_{Nd}(t)$[c]	T_{CHUR} (Ga)[d]
70138,7	A	43.42	0.647	182	0.01020±10	0.699793±14	0.699235±20	5.2	11.5	27.8	0.24990±50	0.514277±10	0.508072±22	6.3±0.4	4.6
71095,6	A	63.73	1.44	319	0.01300±13	0.699951±13	0.699240±20	4.9	25.2	62.3	0.24471±49	0.514164±12	0.508088±24	6.6±0.5	4.8
71539,6	A	36.93	0.787	229	0.009892±98	0.699776±14	0.699235±19	5.2	13.4	32.5	0.25018±50	0.514306±11	0.508094±23	6.7±0.6	4.7
Type A weighted average initials							0.699237±11						0.508084 ±13	6.5±0.3	
70139,6	B1	66.90	0.281	146	0.005515±55	0.699511±14	0.699214±17	6.0	5.30	12.3	0.26021±52	0.514547±11	0.508191±24	7.0±0.5	4.5
repeat		65.28	0.282	146	0.005542±55	0.699518±17	0.699220±20	6.0	5.38	12.4	0.26234±52	0.514605±15	0.508197±28	7.2±0.5	4.5
Type B1 weighted average initials							0.699216±13						0.508194±18	7.1±0.3	
71069,10	B2	43.60	0.315	146	0.006216±62	0.699529±12	0.699195±15	5.5	7.35	17.3	0.25663±51	0.514406±13	0.508138±26	6.0±0.5	4.4
71097,5	B2	28.49	0.293	109	0.007747±77	0.699635±12	0.699218±16	5.4	6.61	16.6	0.24141±48	0.514028±12	0.508131±24	5.9±0.5	4.7
71545,4	B2	49.61	0.354	120	0.008497±84	0.699676±12	0.699219±17	5.2	6.67	16.5	0.24519±49	0.514057±11	0.508068±23	4.6±0.4	4.4
71576,4	B2	45.75	0.382	127	0.008658±86	0.699669±13	0.699203±18	5.1	7.25	18.2	0.24154±48	0.513996±9	0.508096±21	5.2±0.4	4.6
77516,19	B2	46.77	0.340	110	0.008913±89	0.699619±17	0.699140±22	4.6	6.39	15.5	0.24944±48	0.514130±60	0.508037±72	4.0±1.4	4.3
78586,7	B2	46.81	0.389	129	0.008637±86	0.699704±18	0.699239±23	5.4	7.58	18.6	0.24637±49	0.513989±10	0.507971±22	2.7±0.4	4.1
74247,6	C	43.76	1.13	155	0.02103±21	0.700442±13	0.699301±24	4.7	9.36	22.8	0.24764±50	0.514232±05	0.508133±17	6.7±0.3	4.7
74255,31	C	57.98	1.19	160	0.02143±21	0.700436±13	0.699274±25	4.6	9.79	23.9	0.24821±50	0.514244±13	0.508131±25	6.6±0.5	4.7
74275,100	C	59.96	0.864	116	0.02140±21	0.700458±14	0.699297±26	4.6	9.24	22.5	0.24857±50	0.514264±10	0.508142±22	6.9±0.4	4.7
74285,5	C	54.43	1.22	164	0.02142±21	0.700446±13	0.699284±25	4.6	9.96	24.4	0.24644±49	0.514204±24	0.508135±36	6.7±0.7	4.7
74287,5	C	67.25	1.12	148	0.02188±22	0.700471±13	0.699284±25	4.6	9.38	22.8	0.24934±50	0.514278±12	0.508137±24	6.8±0.5	4.7
Type C weighted average initials							0.699288 ±11						0.508135±10	6.7±0.2	

Conditions and methods same as those in Table 1.

[a] Initial Sr and Nd isotopic ratios calculated at 3.75, 3.69 and 3.72 Ga for Type A, B1/B2 and C basalts, respectively, using ^{87}Rb decay constant = 1.42×10^{-11} yr^{-1} and ^{147}Sm decay constant = 6.54×10^{-12}.

[b] Model age relative to I(Sr) = LUNI = 0.69903 (NYQUIST et al., 1974; SHIH et al., 1986). $T_{LUNI} = 1/\lambda * \ln[(^{87}Sr/^{86}Sr - 0.69903)/^{87}Rb/^{86}Sr) + 1]$.

[c] Initial ε_{Nd} calculated at 3.75, 3.69 and 3.72 Ga for Type A, B1/B2 and C basalts, respectively, using present-day chondritic values of $^{143}Nd/^{144}Nd$ = 0.512638 and $^{147}Sm/^{144}Nd$ = 0.1967.

[d] Model age relative to CHUR reservoir using present-day chondritic values listed above. $T_{CHUR} = 1/\lambda * \ln[((^{143}Nd/^{144}Nd - 0.512638)/(^{147}Sm/^{144}Nd - 0.1967)) + 1]$.
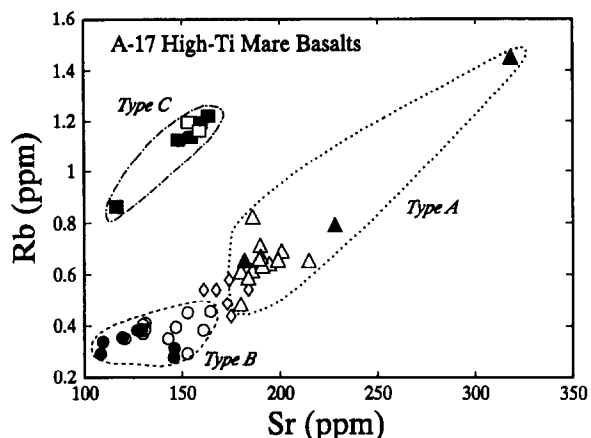
FIG. 5. Whole-rock concentration data determined by isotope dilution techniques for Apollo 17 mare basalts dated by the Rb-Sr method. Filled symbols represent data obtained in the present study; open symbols represent data from previous studies (see Table 2 for sources). Triangles represent rocks classified as Type A basalts, circles as undifferentiated Type B basalts (B1 and B2), and squares as Type C basalts. Open diamonds represent lavas with Rb-Sr compositions intermediate between Types A and B.

Variations in initial isotopic compositions between geochemical groups cannot be solely explained by differences in the eruptive ages proposed above. On a plot of initial ϵ_{Nd} versus I(Sr) (Fig. 6), Types A and C basalts form tight clusters with non-distinguishable initial ϵ_{Nd} values, but with distinct I(Sr) ratios. The unique Sr-Nd isotopic characteristics for these two groups are particularly well-defined if the weighted average initial compositions and resulting uncertainties are compared (Table 3, and shaded error boxes in Fig. 6). Although the field for Type B1 basalts is presently defined by only two analyses of sample 70139, it is largely resolved from the fields for Type A and C basalts. Some overlap between the Type A and B1 fields might be expected if additional analyses show excessive scatter. However, present data from Types A, B1, and C basalts indicate that combined initial Sr-Nd isotopic compositions for these three groups were unique, exhibiting a relatively restricted range in initial ϵ_{Nd} with a somewhat larger range in I(Sr). Differences in initial ϵ_{Nd} between these three groups are strongly dependent on the choice of eruptive ages used in the calculation; however, I(Sr) variations remain distinct regardless of the range of Apollo 17 mare basalt ages. This point is illustrated in Fig. 6 which also includes ϵ_{Nd} and I(Sr) compositions for Types A and B1 basalts calculated at average age of Apollo 17 volcanism (i.e., 3.72 Ga; open triangles and small circles, respectively). Although ϵ_{Nd} compositions become indistinguishable at this age, differences in I(Sr) compositions between the three groups become slightly better resolved.

Initial isotopic compositions for Type B2 basalts are clearly resolvable from the weighted average compositions for Types A, B1, and C lavas. Type B2 lavas show a wide variation in initial isotopic compositions which is well outside of analytical uncertainties (large open circles, Fig. 6). The greatest variations are observed in initial ϵ_{Nd} values which are all lower than that observed in 70139; however, I(Sr) compositions trend towards both higher and lower values relative to 70139.

These isotopic differences might be used as criteria to further discriminate between Types B1 and B2 basalts. Although early work recognized that Type B basalts formed a continuum on many chemical variation diagrams (WARNER et al., 1975, 1979; RHODES et al., 1976), NEAL et al. (1990a) found that these basalts formed two sub-groups on the basis of REE ratios. Both 70139 and 71069 were previously classified as Type B1 basalts according to the elemental criteria outlined by NEAL et al. (1990a) and plot at either end of their B1 field (Fig. 1). However, the initial isotopic compositions of 71069 are outside of 70139 analytical errors and are more characteristic of the other Type B2 lavas. Although differences in isotopic compositions between these two basalts may be attributable to incorrectly assuming a common age for both rocks, this explanation cannot account for the scatter observed in other B2 basalts (see explanation of dashed lines in Fig. 6). Additionally, the La/Sm ratio for 71069 is lower than the values observed for the relatively smooth, sub-horizontal trend defined by 70139 and the Types A and C lavas (heavy dashed line, Fig. 1). Isotopic data imply that 71069 has more affinities with other Type B2 basalts and suggest that it may represent a continuation of the steeply sloping trend of La/Sm versus La defined by Type B2 samples containing higher La/Sm. These data indicate that the discrimination between relatively unevolved Types B1 and B2 basalts with low La/Sm may be difficult on the basis of trace-element chemical data alone.

Whole-Rock Isochrons

Types A, B1, and C whole-rock compositions form well-defined linear arrays on Sr and Nd isochron plots (Fig. 7) in spite of the observations that each group exhibits distinct isotopic characteristics. These arrays cannot be caused by
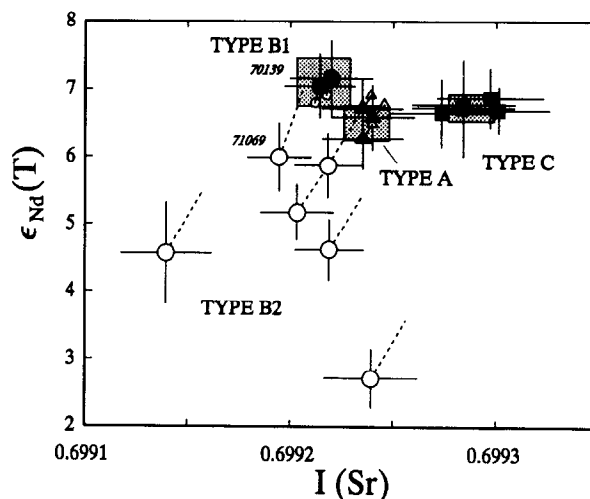

FIG. 6. ϵ_{Nd} versus I(Sr) calculated at the estimated age of eruption for Types A (3.75 Ga; filled triangles), B (3.69 Ga; filled circles, Type B1; open circles, Type B2) and C (3.72 Ga; filled squares) basalts. Shaded boxes represent error limits of weighted averages for each group. Also shown are the initial ratios for Types A and B basalts calculated at the average age of Apollo 17 volcanism for comparison (3.72 Ga; small open triangles and circles, respectively, with tie-lines), and the effects of age correction if B2 samples are younger than the B1 basalt analyzed (dashed lines calculated from 3.69 to 3.56 Ga).

simple, two-component mixing since consistent linear trends are not observed on other bivariate elemental plots (e.g., non-linear Rb-Sr arrays in Fig. 5). In addition, consistent two-component endmembers cannot be defined on the basis of major- and trace-element concentrations; for instance, Type C basalts have La and Sr contents intermediate between Types A and B1, but have the highest Rb, MgO, and Cr contents (NEAL et al., 1990b). Since mixing cannot explain the well-defined linear arrays of whole-rock isotopic data, they should be assessed as isochrons which may preserve time significance. Type B2 analyses show excessive scatter in Fig. 7, particularly on the Sm-Nd isochron plot where two samples plot completely off of the diagram. The wide range of initial isotopic ratios calculated for Type B2 basalts indicates that they no longer (if ever) satisfy the requirement for closed-system evolution from a common initial composition. Therefore, they are not included with the Types A, B1, and C regressions. The resulting Rb-Sr whole-rock regression, including two B1, three A, and five C analyses, yields an age of 4.02 ± 0.05 Ga ($\lambda^{87}Rb$ = 1.42 × 10^{-11} yr^{-1}). This Rb-Sr age is much more precise than internal isochrons determined from individual rocks, even though the range of $^{87}Rb/^{86}Sr$ for the whole rocks is substantially reduced. The higher precision is, in part, the statistical result of regressing a larger number of samples, but

can also be attributed to the higher analytical precision of whole-rock determinations and a smaller amount of scatter of individual analyses about the best-fit curve. The cluster of five, isotopically similar Type C analyses heavily weighs the upper end of the line, strongly influencing the resulting age and, potentially, the associated uncertainty. In order to assess this control, weighted averages of the present-day $^{87}Rb/^{86}Sr$ and $^{87}Sr/^{86}Sr$ values could be calculated; however, this would introduce additional uncertainties in the averaged values caused by small, but real, variations in the Rb/Sr introduced in the different samples at the time of crystallization. Instead, measured values of samples which most closely represent the average composition are regressed and result in ages of 4.01 ± 0.08 Ga if only 74285 is used, and 4.03 ± 0.07 Ga if both 74285 and 74287 are used. These age uncertainties are slightly larger than the 0.05 Ga value calculated for all ten analyses, but are still remarkably precise given the small range in Rb/Sr in these rocks. The low age uncertainties for these regressions indicate that the 4.02 Ga whole-rock Rb-Sr age does not represent a "two-point" isochron and also suggest that although individual mineral phases (particularly, any adhering mesostasis) may have been subjected to slight disruption of the Rb-Sr system, whole rocks remained closed to Rb or Sr flux on the scale of basalt fragment sizes (200–750 mg). Ironically, the more-precise Rb-Sr whole-rock isochron age is 270 to 330 Ma older than the eruptive age of the basalts. In contrast, the less-precise Sm-Nd whole-rock isochron age of 3.79 ± 0.15 Ga is nearly identical to the eruptive age of the Type A magmas, and within error of the eruptive age of the Type B1/B2 basalts. The validity of the whole-rock isochron ages and their implications on models of cumulate source heterogeneity are discussed in the next section.

DISCUSSION

Open-System Evolution vs. Source Heterogeneity

Isotopic data presented earlier support the classification of Apollo 17 high-Ti mare basalts into previously defined geochemical groups. The unique isotopic characteristics of each geochemical basalt-type could not have been acquired from a common mantle source through closed-system magmatic processes (i.e., partial melting and fractional crystallization). However, post-melting, open-system processes, such as fractionation combined with assimilation of KREEP or lunar crust (SHIH et al., 1986; NEAL et al., 1989), are capable of modifying isotopic compositions and must be investigated as a potential cause for the observed isotopic variations.

Type A magmas show very little isotopic variation over a large range of Sr and Nd concentrations (Fig. 8). The absence of plagioclase as a microphenocryst phase, as well as observed CaO, Al_2O_3, and Eu abundances and CaO/Al_2O_3 ratios, indicate that plagioclase was not a major fractionating phase during petrogenesis of any of the Apollo 17 high-Ti magmas (WARNER et al., 1975, 1979; RHODES et al., 1976; NEAL et al., 1990a). Consequently, observed Sr and Nd isotopic and concentration data are compatible with a closed-system, near-surface fractionation model where the remaining liquid would become progressively enriched in both of these incompatible elements while isotopic compositions remained constant. The
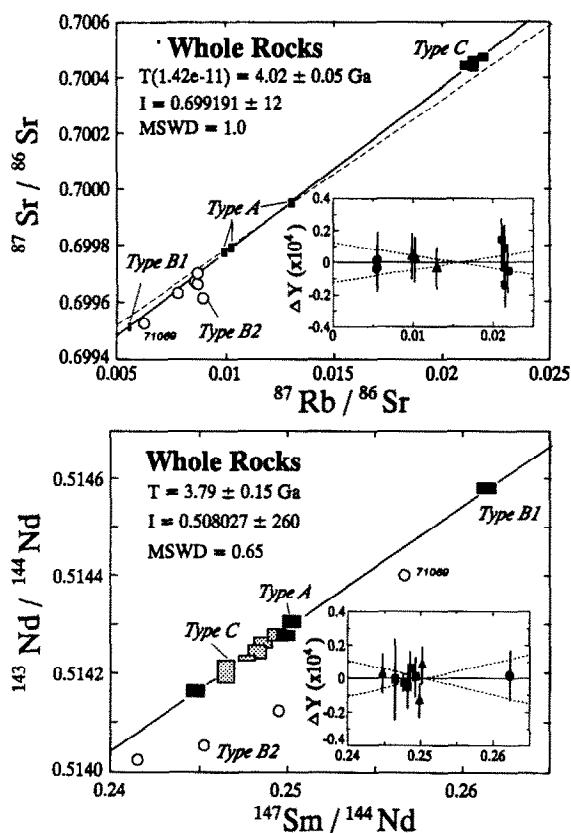

FIG. 7. Rb-Sr and Sm-Nd isochron plots for whole-rock data listed in Table 3 (Sr isochron age = 4.11 Ga using $\lambda^{87}Rb$ = 1.39 × 10^{-11} yr^{-1}). Data from Type B2 basalts (open circles) scatter off of the linear arrays defined by Types A, B1, and C basalts and are not included in the regression analysis. Light dashed line in (a) represents mineral isochron for Type A basalt, 71539. Details listed for Fig. 2 apply equally to Fig. 7.
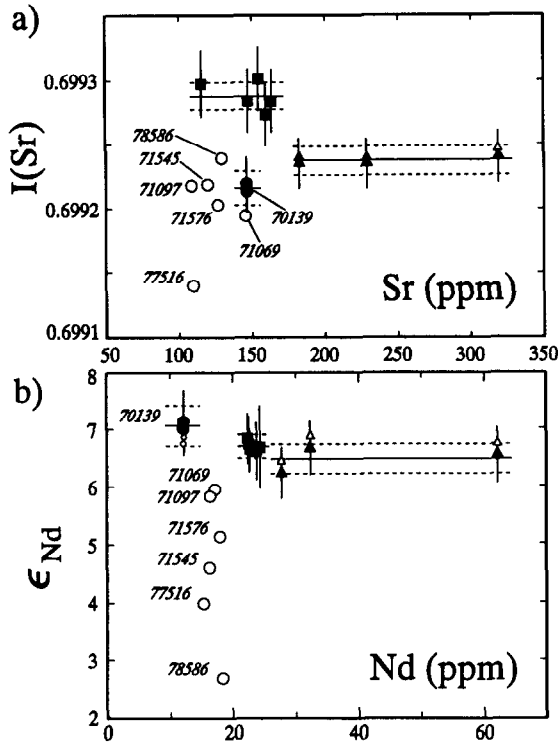
a)

b)

FIG. 8. Initial isotope ratio (calculated at their age of eruption) versus element plots for whole-rock data listed in Table 3. Same symbols as in Fig. 6. Also shown are weighted average isotopic compositions (solid horizontal lines) and 95% confidence limits (dashed lines) for Types A, B1, and C basalts.

observation that both 70138 and 71095 whole-rock analyses fall on 71539 internal Sr and Nd isochrons (Fig. 3) lends strong support to closed-system evolution of Type A magmas. NEAL et al. (1990a) were able to apply closed-system, Rayleigh fractionation models to Type A basalts which require 40–80% crystallization of a hypothetical mafic parent to produce the range of observed derivative-magma compositions. In addition, the most-evolved Type A basalt analyzed in this study (71095) was noted as the only example of a Type II, Apollo 11 low-K type high-Ti basalt recognized in the Apollo 17 suite (NEAL et al., 1990a). The nearly identical initial isotopic composition of this and the other two Type A basalts implies a direct genetic link to a common parental magma through extreme amounts of fractionation.

Unlike Type A magmas, Type C magmas show a tight clustering of Sr and Nd concentrations, as well as isotopic compositions (Fig. 8). Other elemental abundances show equally limited ranges within the recognized Type C suite (NEAL et al., 1990b). Type C basalts are exceedingly rare (five of six known samples are analyzed in this study) and their areal distribution appears to be limited to the immediate vicinity of Shorty Crater (RHODES et al., 1976; WARNER et al., 1979; NEAL et al., 1990b). Although they contain higher MgO and Cr abundances than Types A and B basalts, Type C basalts are most notable in their enrichment of Rb (Fig. 4; RHODES et al., 1976; WARNER et al., 1979; NEAL et al., 1990b). The limited ranges of geochemical and isotopic compositions, along with their scarcity, suggest that all Type C

samples may have been derived from a single batch of magma, and possibly even a single lava flow. The petrogenesis of Type C basalts is discussed in greater detail by NEAL et al. (1990b).

In contrast to Types A and C basalts which show no intra-group isotopic variability, Type B2 magmas exhibit a large range in initial isotopic compositions over only small ranges in Sr and Nd concentrations (Fig. 8). Type B2 samples form a distinct, near-vertical trend on a plot of ϵ_{Nd} versus Nd (Fig. 8b). A similar array is not observed when I(Sr) is plotted against Sr; instead, Type B2 samples form a diffuse cluster (Fig. 8a). Although Type B1 70139 plots at the high ϵ_{Nd}-low Nd end of the array in Fig. 8b, there is no obvious I(Sr) relationship between Types B1 and B2 magmas in Fig. 8a. In addition to their variable initial ratios, Type B2 magmas commonly do not fall on whole-rock isochrons defined by Types A, B1, and C magmas (Fig. 7). We interpret the isotopic data as evidence that the Type B2 magmas experienced post-melting, open-system evolution. This conclusion differs from the one recently proposed by NEAL et al. (1990a) who utilized geochemical modelling to demonstrate, on the basis of major and trace elements alone, that Type B2 compositional variations can be adequately explained by closed-system fractionation from a distinct parent magma with elevated La/Sm. Isotopic data presented here argue strongly for a model requiring assimilation of additional contaminants during evolution of Type B2 magmas. In spite of the single trend of ϵ_{Nd} vs. Nd, Type B2 compositional variations cannot be explained through simple, two-component AFC processes using KREEP, or any single crustal component as the assimilant. The pattern and sequence of ϵ_{Nd} depletion observed for Type B2 samples in Fig. 8b is not duplicated on the Sr-Nd isotope plot (Fig. 6), nor on other isotope-element or element-element diagrams. Modelling of AFC processes is also complicated by the difficulty in choosing an appropriate uncontaminated parent magma. While the least-evolved (i.e., highest MgO, Cr_2O_3, Sm/Nd, lowest La, Hf, Rb/Sr) Type B1 magma, 70139, cannot be ruled out, its I(Sr) and La/Sm are intermediate within the range of Type B2 compositions. Given the limited number of analyses in the present study and the uncertainty in assuming a common age for both Types B1 and B2, a detailed examination of Type B2 petrogenesis is not possible at present. However, we suspect that these magmas experienced a complex magmatic history involving several different assimilants, parent magmas, or even source regions in order to explain observed compositions.

In summary, whole-rock isotopic data suggests that the Type B2 basalts were the only Apollo 17 high-Ti magmas which suffered extensive interaction with lunar crust. Type A basalts exhibit the most convincing isotopic evidence in support of closed-system magmatic evolution. Their large range in geochemical compositions requires the presence of at least several flows which presumably evolved in magma chambers at some depth within the lunar crust. It is unlikely that these basalts could have acquired their highly evolved geochemical compositions while maintaining their uniform initial isotopic signatures if they suffered any concurrent crustal assimilation. Therefore, Type A isotopic compositions are inferred to have been inherited from their mantle source region. Although similar strong evidence is lacking for Types C and B1 magmas, we assume that neither of these two geo-
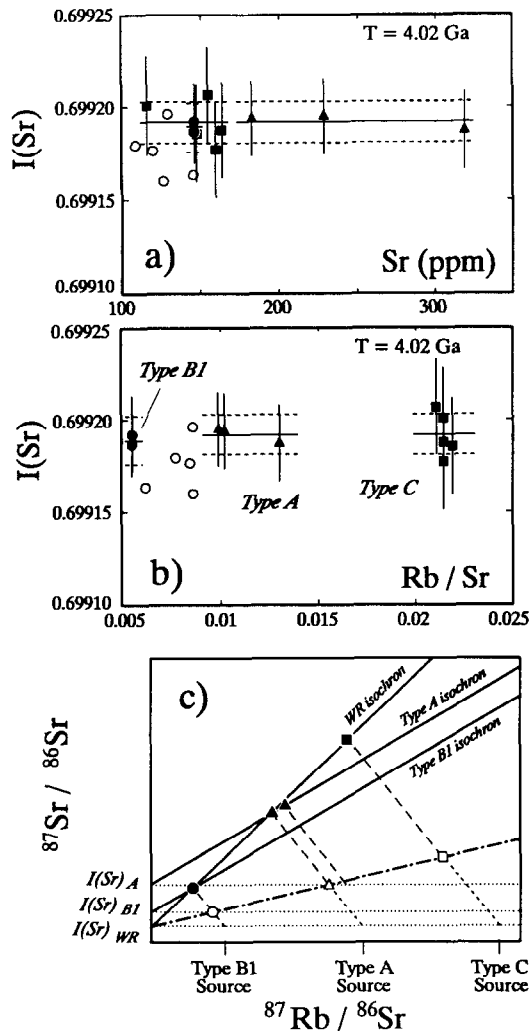
FIG. 9. "Initial" $^{87}Sr/^{86}Sr$ ratios for Types A, B1, and C source regions calculated at 4.02 Ga plotted against (a) Sr concentration and (b) Rb/Sr ratios measured in whole rocks. Also shown are the weighted average initial compositions and error limits for Types A, B1, and C basalts which are essentially identical. (c) Schematic diagram illustrating the growth of $^{87}Sr/^{86}Sr$ with time in whole rocks. At 4.02 Ga, all three sources have a common $I(Sr)_{WR}$, but a range of recently modified $^{87}Rb/^{86}Sr$ ratios. At around 3.7 Ga (dash-dot isochron), basalts are generated and preserve the $^{87}Rb/^{86}Sr$ and initial ratios inherent in their respective source regions (open symbols and dotted lines at $I(Sr)_{B1}$ and $I(Sr)_A$). Minor Rb/Sr fractionation during melting, or very high degrees of crystallization, or magma mixing, may cause some increases in $^{87}Rb/^{86}Sr$ (e.g., two values for Type A). Present-day basalt compositions are shown as solid symbols and lie both on parallel 3.7 Ga mineral isochrons and on the steeper 4.0 Ga whole-rock isochron (solid, bold lines). Note similarities to Type A and whole-rock isochrons shown in Fig. 7a.

chemical groups experienced significant crustal assimilation. This assumption is supported by the fact that neither magma type exhibits the intra-group isotopic variability observed in Type B2 magmas and, more importantly, by the fact that data for both Types C and B1 plot on the whole-rock Nd isochron defined by Type A basalts alone. The resulting age of 3.79 Ga for the Nd whole-rock isochron (nearly identical to the age of eruption of Type A basalts) and the discordance

of contaminated Type B2 magmas provide additional support for assuming that Types A, B1, and C evolved under closed-system conditions. In addition, differences in initial isotopic compositions between these three groups indicate that Types A, B1, and C parent magmas were distinct and that primary magmas for each geochemical group were derived from isotopically unique mantle sources. Thus, isotopic data presented in this paper support previous petrogenetic interpretations based on major- and trace-element geochemistry which involved relatively simple fractionation of observed microphenocryst phases from compositionally distinct source regions (NEAL et al., 1990a). Isotopic evidence suggesting that B2 melts were modified by crustal contamination eliminates much of the need for previously proposed models (SHIH et al., 1975; WARNER et al., 1979) requiring differing degrees of partial melting in order to explain observed compositional variations (e.g., La/Sm ratios).

Origin of Source Heterogeneities

Whole-rock isotopic data for Types A, B1, and C basalts present an apparent conflict between the Sr and Nd systems. On the one hand, variations in initial Nd isotopic data are largely a result of the time-integrated effects of the similar Sm/Nd ratios calculated at different eruptive ages. Variations in $^{147}Sm/^{144}Nd$ ratios between the three different groups is only about 5%, and the Nd whole-rock isochron (Fig. 7b) yields an age almost identical to the average eruptive age. These observations suggest that source regions for each group contained only minor differences in REE distributions and Nd isotopic compositions.

On the other hand, Sr data indicate that each mantle source is isotopically distinct. Age versus initial Sr composition error parallelograms for 70139 (Type B1) and 71539 (Type A) (Fig. 10a), as well as non-overlaping I(Sr) errors for Type C basalts (Fig. 6), define unique source characteristics. Even though the different basalts record Sr isotopic heterogeneities in their respective sources, the Sr whole-rock data yield a well-defined, albeit anomalously old, age of 4.02 ± 0.05 Ga. Taken at face value, this implies that all three Apollo 17 mare basalt sources had a homogeneous $^{87}Sr/^{86}Sr$ composition of 0.699191 ± 0.000012 at 4.02 Ga. It is unlikely that this age represents the time at which mantle cumulates crystallized from a homogeneous magmasphere since it is some 400 Ma younger than previous estimates of 4.4 Ga (CARLSON and LUGMAIR, 1979; NYQUIST et al., 1979, 1981; TAYLOR, 1982) and would require anomalously slow rates of cooling of the magmasphere (TAYLOR, 1982).

The 4.02 Ga whole-rock Rb-Sr isochron has age significance only if there has been no fractionation of Rb and Sr at the time of melt generation. NYQUIST et al. (1979) have convincingly argued that partial melts derived from a source containing clinopyroxene as a residual phase will contain Rb/Sr ratios which are higher than that of the source due to the difference in Rb and Sr mineral/liquid partition coefficients in Ca-rich pyroxene (0.015 for Rb and 0.116 for Sr: PHILPOTTS and SCHNETZLER, 1970). Since the Rb/Sr fractionation which takes place during partial melting is much smaller than the fractionation which occurred during crystallization of magmasphere cumulates (due to extraction of
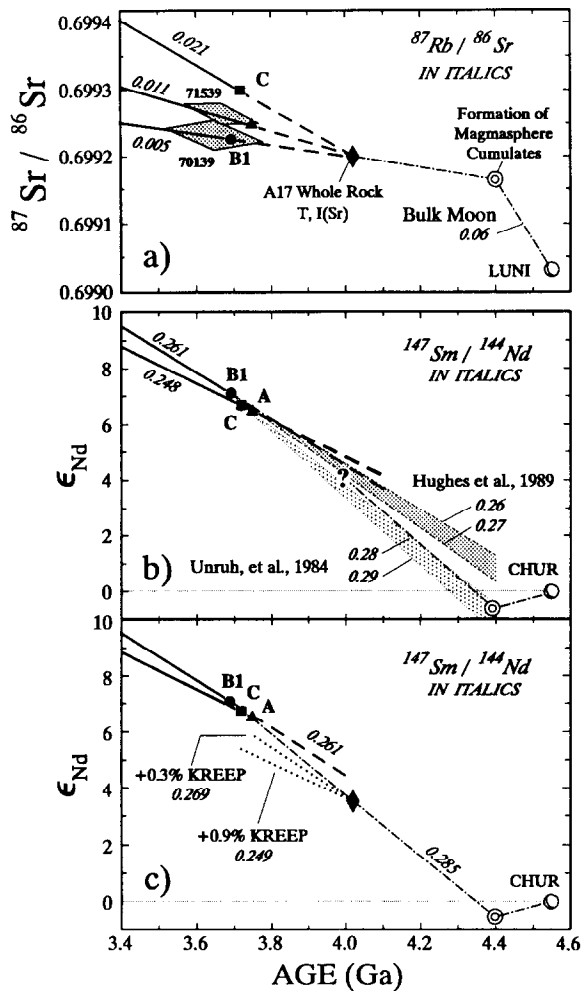
FIG. 10. Isotope evolution diagrams for average Types A, B1, and C mare basalts. Radiogenic growth is projected back to the estimated age of eruption (solid lines) using average present-day isotopic ratios and measured Rb/Sr and Sm/Nd. Extensions of these same evolution paths to 4.02 Ga (i.e., no fractionation of Rb/Sr or Sm/Nd at time of melting) are shown by dashed lines. Also shown are Sr error parallelograms for 71539 and 70139 from isochron determinations (large, stippled polygons), the age and I(Sr) composition of the Rb-Sr whole-rock isochron (filled diamond), and estimated evolution paths for the magmasphere (dash-dot line from LUNI/CHUR to formation of magmasphere cumulates at about 4.4 Ga after previously-proposed models; NYQUIST et al., 1977, 1979, 1981; UNRUH et al., 1984). In (b) Nd isotopic compositions for the Type B1 source are modelled assuming that 70139 represents 10% (lower boundaries of stippled fields) and 15% (upper boundaries) partial melts of original cumulates with modal compositions and mineral partition coefficients given by UNRUH et al. (1984) and HUGHES et al. (1989). Note that the $^{147}Sm/^{144}Nd$ for both Type A and C are identical. In (c) dotted lines show the divergent evolutionary paths for Types A and C source regions assuming that small amounts of KREEP are mixed with original B1 mantle cumulates at 4.0 Ga (mixing model from Table 4).

a plagioclase crust), whole-rock ages should approximate the ages of formation of basalt sources (NYQUIST et al., 1979). However, these authors also argue that *rigorous* source-region time significance cannot be placed in whole-rock isochrons because of the melt-induced Rb/Sr fractionation. Their earlier work with Apollo 17 basalts (NYQUIST et al., 1976) modelled 0.25- to 5-fold increases in Rb/Sr ratios between Type B to

Type C melts and their respective cumulate sources. These results were interpreted as evidence for a two-stage evolution for Apollo 17 cumulate sources involving crystallization at 4.4 Ga of cumulate sources exhibiting a range in $^{87}Sr/^{86}Sr$ compositions followed by closed-system evolution until basaltic liquids were remelted between 3.7 and 3.8 Ga (Fig. 5, NYQUIST et al., 1976).

Several lines of isotopic and petrologic evidence force us to reexamine the extent of Rb/Sr fractionation that occurred during generation of Apollo 17 high-Ti melts. Most importantly, the high degree of precision of the 4.0 Ga whole-rock isochron, relative to other whole-rock regressions, limits the amount of Rb/Sr fractionation which could have occurred at the time of melting. As argued previously, this precision is not an artifact of a large spread in initial $^{87}Rb/^{86}Sr$ values nor of an uneven distribution of analyses (i.e., a two-point isochron). Parallel REE patterns between magma types (NEAL et al., 1990a,b) and relatively constant La/Sm ratios (Fig. 1) indicate similar REE distributions between source regions and comparable degrees in partial melting. If the entire range in Apollo 17 Rb/Sr compositions was derived during partial melting by increasing these ratios in the melts relative to a homogeneous source, the Sr whole-rock isochron should yield an age close to the average age of Apollo 17 volcanism. However, if the sources contained a range of Rb/Sr prior to melting, further melt-induced fractionation of Rb and Sr would only tend to disrupt the linearity of the whole-rock data and increase, rather than decrease, the scatter of points about the best-fit isochron regression. Alternatively, if the cumulate source regions inherited substantial $^{87}Sr/^{86}Sr$ heterogeneity at the time of magmasphere crystallization (e.g., Fig. 5, NYQUIST et al., 1976), the resulting melts should not be expected to form a well-defined isochron array at any time.

The small amount of scatter associated with the Sr whole-rock isochron is also illustrated by initial Sr ratios calculated at 4.02 Ga for individual Types A, B1, and C whole rocks (Fig. 9a and b). Values for I(Sr) fall well within the limits of analytical error between 0.699206 and 0.699185, while both Sr concentrations and Rb/Sr ratios show much broader ranges. Weighted average I(Sr) calculated at 4.02 Ga for all three magma types show a remarkably good agreement of 0.699189 ± 0.000013 for the two analyses of 70139 (Type B1) and 0.699192 ± 0.000011 for the three Type A and five Type C basalts. These data suggest that the range in Rb/Sr ratios was established at around 4.0 Ga at a time when all three source regions had very homogeneous Sr isotopic compositions, and that the Rb/Sr could not have been substantially modified during subsequent melt generation or crystal fractionation without disturbing these relationships. Additionally, the very low values of $^{87}Rb/^{86}Sr$ in 70139 also support a melting model which does not allow fractionation of Rb from Sr. Strontium isotopic evolution paths for the three groups converge at 0.699191 at 4.0 Ga using $^{87}Rb/^{86}Sr$ measured in the basalts (Fig. 10a). However, if the Type B1 path is projected further back in time using its measured $^{87}Rb/^{86}Sr$, it coincidentally intersects the path of previously proposed models for the evolving Bulk Moon at the time of magmasphere crystallization around 4.4 Ga (using LUNI = 0.69903 and $^{87}Rb/^{86}Sr_{BULK\ MOON}$ = 0.06; NYQUIST et al., 1976, 1977, 1981). The internal consistency of our data with

models derived from different data sets provides further evidence that 70139 (Type B1) most likely preserves the originally formed mantle cumulate $^{87}Rb/^{86}Sr$ ratio with little or no modification. Since REE data allow only subtle differences in the degree of melting between Types B1 and C liquids, it does not seem unreasonable that both Type B1 and Type C (as well as Type A) melts would preserve their respective mantle-source Rb/Sr ratios.

Finally, if the variations in $^{87}Rb/^{86}Sr$ ratios between basalt groups are the result of fractionation through varying degrees of partial melting, the magnitude of the Rb/Sr increases should be well correlated with relative decreases in $^{147}Sm/^{144}Nd$ between groups. Although the Type B1 basalt contains the lowest $^{87}Rb/^{86}Sr$ and highest $^{147}Sm/^{144}Nd$, Types A and C basalts have identical $^{147}Sm/^{144}Nd$ ratios (average values of 0.2483 and 0.2480, respectively), but $^{87}Rb/^{86}Sr$ ratios which vary by a factor of 2 (0.011 versus 0.021, respectively). These observations are inconsistent with accepted models of mineral/melt partitioning during progressive partial melting and indicate that enrichments in Rb/Sr cannot be solely attributed to melt-related fractionation.

Isotopic evidence implying a minimal amount of Rb/Sr fractionation during partial melting requires that late-crystallizing cumulus Ca-rich clinopyroxene (as well as any plagioclase) originally present within the source could not have been present as a major phase within the melt residue. Petrologic models based on experimental, major- and trace-element constraints (GREEN et al., 1975; KESSON, 1975; BINDER, 1985; HUGHES et al., 1989) suggest that high-Ti basalt sources are relatively shallow (<400 km) and are probably dominated by early-formed olivine cumulates. A range of cumulate modes and F values (fraction of melt generated) have been postulated, most of which can be made compatible with a residue largely depleted in clinopyroxene. The hybridized source models of HUGHES et al. (1989) hypothesize that late-stage clinopyroxene, ilmenite, and plagioclase cumulates, along with trapped liquid, are likely to have formed only a small proportion of the high-Ti basalt source regions (<12%) and would have been completely consumed during cumulate remelting of between 10 and 15%. This conclusion is also consistent with models based on Nd-Hf isotopic data which suggest clinopyroxene modal abundances of 8-18% in the Apollo 17 source and 3-15% partial melting calculated to produce observed mare compositions (UNRUH et al., 1984). Although these melting models are highly assumption-dependent, we believe that they can be used to support the conclusion that most or all of the Ca-rich clinopyroxene present in the source regions for Apollo 17 high-Ti basalts was exhausted during partial melting, and that Rb/Sr ratios measured in the basalts are not substantially modified from the values which were present within their mantle sources. This conclusion implies that the 4.02 Ga whole-rock Sr age reported earlier has significance in the evolution of the sources of Apollo 17 mare basalts.

Present Sr isotopic data preserve evidence that the mantle source regions experienced a complex geochemical history during the period between solidification of source cumulates from the lunar magmasphere and generation of Apollo 17 mare basalts (Fig. 10a). These data are consistent with a model

where an initial, isotopically homogeneous source region for Apollo 17 high-Ti basalts crystallized during the late stages of lunar magmasphere solidification around 4.4 Ga (HUGHES et al., 1989). This model also accommodates early lunar Sr isotopic evolution based on previous estimates of the Bulk Moon $^{87}Rb/^{86}Sr$ and $I(Sr)_{LUNI}$ (NYQUIST et al., 1977, 1979, 1981). Crystallization of the magmasphere resulted in depletions in LREE and LIL elements within original mantle cumulates. The low $^{87}Rb/^{86}Sr$ ratio of about 0.005 in the initially homogeneous cumulates caused only very slow growth of radiogenic Sr (near horizontal dash-dot line, Fig. 10a). However, a geochemical event at around 4.0 Ga created a two- to four-fold increase in $^{87}Rb/^{86}Sr$ ratios within what would later become the Types A and C basalt sources, respectively, while leaving the Type B1 source unaffected. The new $^{87}Rb/^{86}Sr$ ratios caused the Sr evolution paths for each source region to diverge such that resolvable differences in $^{87}Sr/^{86}Sr$ were developed by the time high-Ti magmas were generated at 3.7 Ga. This evolution is also depicted schematically on an isochron plot (Fig. 9c) illustrating the growth of $^{87}Sr/^{86}Sr$ (short dashed lines) within the three different sources from 4.0 to 3.8 (open symbols and dashed-dot isochron), and subsequent growth within the basalts (long dashed lines) to the present day (filled symbols and solid isochrons).

Unlike the more-ancient, Sr whole-rock isochron, Nd whole-rock data preserve an isochron age of 3.79 ± 0.15 Ga which is nearly identical to the eruptive age of the basalts. This suggests that either the REEs were not affected by the chemical processes which altered Rb/Sr ratios in the mantle cumulates at 4.0 Ga, or that any REE modifications affected only absolute abundances without changing Sm/Nd ratios in the different sources. Although some fractionation of Sm/Nd most likely occurred during generation of the high-Ti basalts (Fig. 10b), present Nd isotopic data place limits on Sm/Nd ratios in the source regions. If magmasphere cumulates had a chondritic to slightly enriched ϵ_{Nd} composition at 4.4 Ga (NYQUIST et al., 1977, 1979; UNRUH et al., 1984), the $^{147}Sm/^{144}Nd$ of a single-stage source region just prior to melting must have been between 0.27 and 0.29 (Fig. 10c). These values are within the range calculated from the basalt melting models in Fig. 10b. If the Type B1 source remained unmodified since crystallization of magmasphere cumulates, as hypothesized from Sr isotopic data, its ϵ_{Nd} evolution would be controlled by a $^{147}Sm/^{144}Nd$ ratio of around 0.286. Types A and C magmas have ϵ_{Nd} values which are nearly coincident with this path at the time of their eruption. This coincidence indicates that modification of Types A and C source regions at 4.0 Ga by a process capable of imparting Rb-enrichments could not have simultaneously introduced a LREE-enriched component. If it had, the time-integrated effects of the altered Sm/Nd ratios in the different sources would have resulted in Types A and C magmas with lower ϵ_{Nd} values than those observed (dotted lines, Fig. 10c). It may be possible that the absolute abundances of all REEs were modified sympathetically by some process leaving REE ratios in the resulting mantle sources unaffected. However this possibility seems unlikely given the wide range of REE patterns expected for processes involving melting, metasomatism, and/or mixing within the lunar mantle. The data presented here suggest that

Table 4: Illustrative mixing model between high-Ti mare basalt source and KREEP components.

	Rb	Sr	$^{87}Rb/^{86}Sr$	$^{87}Sr/^{86}Sr^a$	Sm	Nd	$^{147}Sm/^{144}Nd$	ε_{Nd} ^{a}
End-members:								
B1 Source[b]	0.0406	21.3	0.00551	0.699191	0.756	1.60	0.286	3.00
KREEP[c]	13.4	89.8	0.433	0.699570	22.6	80.9	0.169	-0.61
B1 Source-KREEP Mixture:								
% KREEP								
0.33	0.0848	21.5	0.0114	0.699192	0.827	1.86	0.269	2.99
0.92	0.163	21.9	0.0215	0.699194	0.956	2.32	0.249	2.97
Observed:								
Type A Magma			0.0114				0.247	
Type C Magma			0.0215				0.248	

[a] Isotopic compositions at 4.0 Ga

[b] B1 Source calculated assuming 70139 represents a 15% non-modal melt using the following
parameters modified from UNRUH, et al. (1984), and HUGHES, et al., (1989):

	Olv	Opx	Cpx	Other
Modal proportions	0.65	0.21	0.07	0.07
Melt proportions	0.05	0.05	0.45	0.45

where "Other" equals plagioclase + ilmenite + phosphate + trapped liquid. Both Cpx and
"Other" phases become exhausted from the residue at 15% melting. Mineral distribution
coefficients for Olv and Opx are from UNRUH, et al. (1984). Values for $^{87}Rb/^{86}Sr$ and
$^{147}Sm/^{144}Nd$ of 0.00551 and 0.286, respectively, in the B1 source are assumed and
concentrations are modified slightly to obtain these ratios.

[c] Trace elements are an average of 18 Apollo 17 KREEP analyses reported by SALPAS, et al. (1987).
Isotopic compositions are from SHIH, et al. (1990).

a geochemical process is required which is capable of im-
parting an up to four-fold increase in the Rb/Sr ratio of Type
C source region relative to Type B1 source region without a
concomitant modification of REE ratios.

Strontium and neodymium arguments considered together
help to establish the nature of the event which affected the
Sr isotopic systematics of Types A and C mantle sources at
4.0 Ga. KREEPy basaltic magmatism identified at the Apollo
17 site occurred at the same time that high-Ti mare basalt
sources were modified (COMPSTON et al., 1975; SHIH et al.,
1990). Ages between 4.01 and 4.13 have been reported with
I(Sr) of 0.69954 to 0.69960 and ε_{Nd} of −0.61 (SHIH et al.,
1990). Although it is possible that injection of a KREEP
magmatic component into the original LIL- and LREE-de-
pleted cumulate source region may have caused some mod-
ification, it is difficult to reconcile both Sr and Nd isotopic
data through a KREEP mixing model. To illustrate these
inconsistencies, Rb, Sr, Sm, and Nd contents for unmodified
B1 source are estimated in Table 4. These concentrations are
poorly constrained; however, they should be reasonable
enough to model the effects of addition of KREEP. Because
the abundances of these elements are so low in the B1 source
and so high in KREEP, addition of only 0.33 and 0.92% of
the KREEP endmember is capable of reproducing $^{87}Rb/^{86}Sr$
ratios assumed for Types A and C source regions. Even though
isotopic compositions of the two components are quite dif-
ferent, the isotopic compositions of the mixed sources are
not noticeably shifted from that of the B1 source due to the
very small amounts of KREEP added. However, the effect
of this mixing model on the $^{147}Sm/^{144}Nd$ is sufficient to cause
a substantial deviation in the evolution of Nd isotopes during
the 270 to 330 Ma between source modification and melt
generation (dotted lines, Fig. 10c). Not only should the ε_{Nd}

values in the Types A and C sources be lowered from around
+6.6 to +5.4 and +4.5, respectively, but also, the higher pro-
portion of KREEP added to the Type C source should cause
a dispersion of ε_{Nd} values in Types A and C sources with
time. Instead, the isotopic composition of both sources are
nearly identical and lie along the Type B1 source evolution
path. The Nd isotopic systematics in Types A, B1, and C
basalts combined with the LREE-enriched patterns common
to KREEP-rich rocks create a fundamental problem in all
KREEP-mixing models regardless of specific choices for either
original mantle cumulate or KREEP compositions. Similar
arguments can be made involving small degrees of partial
melting either added to or subtracted from the mantle cu-
mulates. Although small amounts of melting will cause frac-
tionation of Rb from Sr, this process is also very effective at
fractionating Nd from Sm.

Other, more Rb/Sr-enriched *magmatic* components which
could have been mixed into the original cumulate source are
either immiscible granite melts (RUTHERFORD et al., 1976;
SHIH et al., 1985; TAYLOR et al., 1980; WARREN et al., 1983)
or a hypothetical K-Fraction melt derived through silicate
liquid immiscibility in evolved KREEP (NEAL and TAYLOR,
1989). These types of K-rich magmas have extremely high
Rb abundances and Rb/Sr ratios, on the order of 100–200
ppm and 1, respectively. As a consequence, only a very mi-
nute amount of this material is required (less than 0.1%) to
elevate Rb/Sr ratios in Types A and C source regions. Al-
though these materials have LREE-enriched patterns similar
to KREEP, the somewhat lower REE abundances along with
the very low mixing proportions may result in only negligible
changes in the $^{147}Sm/^{144}Nd$ of the hybrid sources. Therefore,
these components are potentially capable of imparting sig-
nificant Rb/Sr modification without substantial Sm/Nd ef-

fects. However, the viscosity of these highly polymerized magmas (approximately 3×10^4 poise; NEAL and TAYLOR, 1989) make it difficult to envisage a mechanism of physically mixing the very small amounts of infiltration required to modify Types A and C sources.

Another mechanism capable of modifying the original mantle cumulates involves mobilizing Rb and other volatile metals preferentially to incompatible, but refractory, elements such as the REEs. The presence of volatile elements enriched on the surfaces of lunar glass spheres, thought to be of pyroclastic origin, has been interpreted as evidence for the volatile transport (especially as halogen complexes) of metals (CHOU et al., 1975; MEYER et al., 1975). DICKINSON et al. (1989) have proposed that halogen-rich vapors were responsible for redistributing Ge within the lunar interior resulting in a form of mantle metasomatism. Their model speculates that volatile elements, including Ge, were leached from wall rocks by F- and Cl-rich fluids originating from outgassing of the lunar interior. Volatile metals, complexed with halogens, were transported outward until they encountered more-siliceous, Na- and K-rich magmas (i.e., urKREEP) where the halogen complexes were then resorbed into the KREEPy magmas due to the higher solubility of Cl and F in alkaline silicate liquids. A similar gas/fluid transport model can be invoked to explain the Rb/Sr differences between Apollo 17 mare basalt sources. The ability of volcanic gases to transport volatile metals has been shown at numerous active terrestrial vents (ZOLLER et al., 1983; SYMONDS et al., 1987; CROWE et al., 1987). Alkali metals are highly enriched in these gas and sublimate samples relative to both their abundances in the associated silicate melts, as well as to Sr and REE abundances within the same volcanic gases. In typical terrestrial volcanic gases where Cl has a higher fugacity relative to F, the alkali metals Cs, Rb, K, and Na, are all stable as chloride complexes rather than as F, Br, OH, elemental, or other gas species (SYMONDS and REED, 1991). Therefore, it is conceivable that Cl-rich fluids, derived through outgassing of the lunar interior, or through final crystallization of KREEPy magmas emplaced at mantle-source depths, were capable of leaching and transporting substantial amounts of Rb with little or no mobilization of either Sr or the REEs. Although REEs may be fractionated by this process, the absolute abundances of REEs transported by these fluids will most likely be small relative to the amount of Rb in solution. It is also probable that Cl-rich fluids have very low viscosity, allowing even small amounts of this geochemical component to infiltrate into the original mantle cumulates.

Processes involving halogen-rich metasomatism provide an attractive means of explaining the disruption of the Rb-Sr system in Apollo 17 high-Ti basalts while leaving the Sm-Nd system intact. Equally important, it also allows modification of the Rb/Sr ratios without altering the $^{87}Sr/^{86}Sr$ compositions within the different sources so that a common I(Sr) at 4.02 Ga remains well defined. Further evidence for a metasomatic origin for the Rb/Sr heterogeneities may be recorded by Ge concentrations, which are three times higher in Type C basalts relative to the other Apollo 17 magma types (DICKINSON et al., 1989). Since Ge bulk distribution coefficients are close to unity in mantle assemblages, abun-

dances measured in basalts should be representative of their mantle sources (DICKINSON et al., 1989). The observed Ge disparity may have been introduced at the same time that Rb/Sr ratios were modified, and may be linked, in some manner, to the similar-aged, Ge-enriched KREEPy basalts sampled at the Apollo 17 site. Ultimately, a fluid-infiltration model will require explanations for the mechanisms controlling the precipitation of transported metals from these fluids, as well as a reason for the progressive increase of fluid contributions into Types A and C source regions, respectively. Although details of lunar metasomatism are not yet clear, we speculate that this type of process played an important role in establishing the geochemical and subsequent isotopic heterogeneities observed in Apollo 17 high-Ti mare basalts.

CONCLUSIONS

Combined Sr and Nd isotopic studies of well-documented mare basalt suites offer the potential to refine details of basalt chronology and petrogenesis which are not wholly apparent from geochemical or single-system isotopic studies. In the present case, previously defined geochemical types of Apollo 17 high-Ti basalt (Types A, B1, B2, and C) exhibit slight differences in age which help to establish a geochemical stratigraphy, as well as subtle variations in initial isotopic compositions which permit characterization of different styles of magmatic evolution, distinction of source heterogeneities, and models for the geochemical histories of cumulate sources.

Two new internal Sr and Nd isochron ages presented in this study do not allow resolution between Type A and Type B1 eruptive ages (3.75 ± 0.07 Ga for 71359, and 3.71 ± 0.12 Ga for 70139, respectively) given the level of errors associated with regression calculations and the uncertainty surrounding the choice of a ^{87}Rb decay constant. However, utilization of the larger Apollo 17 mare basalt chronological data set offers the potential for reducing the uncertainties in average ages for the different chemical groups. Statistical treatment of all available Apollo 17 mare basalt dates suggests a weighted average age of volcanism of 3.72 ± 0.04 Ga. However, if the dated basalts are classified on the basis of chemical criteria, a resolvable difference in ages between Types A (3.75 ± 0.02 Ga, N = 4) and Types B1/B2 (3.69 ± 0.02 Ga, N = 3) is observed (Fig. 4). Type C basalts cannot be placed into this present chronological sequence with any certainty given the available data. Therefore, Apollo 17 mare basalt volcanism was dominated by early eruptions of Type A magmas, whereas later, magmatism consisted predominantly of Type B1/B2 magmas. Without the ability to clearly resolve age differences between individual flows, the nature of the transition between early and late magmatism remains unclear. Eruption of mare basalts may have been a more-or-less continuous event lasting for a period of 70 to 150 Ma and implying that Types A and B1/B2 magmas may have been produced contemporaneously over at least part of this age interval. Conversely, generation of Types A and B1/B2 magmas may have been temporally discrete with a substantial time hiatus separating generation and eruption of the two magma types. The ability to discriminate between these two eruptive scenarios has important implications for mechanisms of melt generation and may be addressed by additional dating of well-characterized samples.

Whole-rock isotopic results confirm previous petrogenetic hypotheses which proposed that compositional variations *within* Types A, B1, and C geochemical groups can be explained by closed-system fractional crystallization of observed microphenocrystic phases (NEAL et al., 1990a). In contrast, Type B2 lavas exhibit a wide range of intra-group isotopic variation. Observed variations in initial isotopic composition cannot be ascribed to a simple two-component mixing model and are therefore qualitatively explained by assimilation of several isotopically distinct crustal components during transit of magmas to the surface. Recognition of assimilation–fractional crystallization processes in Type B2 magmas may eliminate much of the need for previously proposed models invoking variable degrees of partial melting to explain the range of La/Sm in Apollo 17 magmas (SHIH et al., 1975; WARNER et al., 1979).

Subtle variations in isotopic compositions observed *between* Types A, B1, and C magmas are best explained by heterogeneities within the source regions for each basalt type. Source heterogeneities have been proposed previously on the basis of geochemical data (SHIH et al., 1975; WARNER et al., 1975, 1979; RHODES et al., 1976; NEAL et al., 1990a); however, present isotopic data allow constraints to be placed on the geochemical history of the Apollo 17 mantle sources. Whole-rock Sr data preserve a very well-defined isochron age of 4.02 ± 0.05 Ga ($\lambda^{87}Rb = 1.42 \times 10^{-11}$ yr^{-1}) and initial Sr isotopic composition of 0.699191 ± 0.000012. Although minor melting-induced modification of $^{87}Rb/^{86}Sr$ ratios cannot be completely dismissed, cumulative isotopic evidence, plus the presence of similar-aged KREEPy basalts at the same site, lead us to place geological importance in the whole-rock Sr isochron age. This date is interpreted to represent the last time at which the source regions for Types A, B1, and C magmas contained a common Sr isotopic composition resulting from the closed-system growth of radiogenic Sr in the LIL- and LREE-depleted mantle cumulates which crystallized around 4.4 Ga from the lunar magmasphere. In contrast, whole-rock Nd data from Types A, B1, and C basalts define an isochron age of 3.79 ± 0.15 Ga which is within error of the eruptive ages. This observation requires strong similarities in Nd isotopic compositions between the three groups and indicates that the Sm-Nd systems were not similarly disturbed around 4.0 Ga. Although KREEP magmatism with ages between 4.01 and 4.13 Ga has been identified at the Apollo 17 site (COMPSTON et al., 1975; SHIH et al., 1990), combined Sr and Nd isotopic data are not consistent with KREEP-cumulate mixing models. Instead, a mixing component with higher Rb abundances relative to Sr and the REEs is required. Although lunar granite or the "K-fraction" of KREEP (NEAL and TAYLOR, 1989) are potential candidates, we prefer a model of mantle metasomatism involving halogen-rich fluids derived either through outgassing of the lunar interior or through final crystallization of KREEPy magmas emplaced nearby. These types of fluids are likely to be efficient at mobilizing volatile metals, such as Rb, but much less capable of transporting either Sr or the more-refractory REEs. This type of process is capable of explaining the inhomogeneous introduction of Rb into an originally homogeneous Apollo 17 high-Ti mare basalt source region at around the same

time that KREEP magmatic activity occurred at the Apollo 17 site. After alkali metasomatism, Sr isotopic compositions in the different source regions evolved divergently as a response to modified Rb/Sr ratios, while Sm/Nd remained undisturbed and Nd isotopic evolution within each source remained parallel until mare basalts were generated around 3.7 Ga. Further geochemical investigation of volatile element abundances within these three magma types may provide additional support for this metasomatic model.

REFERENCES

BINDER A. B. (1985) The depths of the mare basalt source region. *Proc. 15th Lunar Planet. Sci. Conf.; J. Geophys. Res.* **89**, C396–C404.

BROWN G. M., PECKETT A., EMELEUS C. H., PHILLIPS R., and PINSENT R. H. (1975) Petrology and mineralogy of Apollo 17 mare basalts. *Proc. 6th Lunar Sci. Conf.*, 1–13.

CARLSON R. W. and LUGMAIR G. W. (1979) Sm-Nd constraints on early lunar differentiation and the evolution of KREEP. *Earth Planet. Sci. Lett.* **45**, 123–132.

CHOU C.-L., BOYNTON W. V., SUNDBERG L. L., and WASSON J. T. (1975) Volatiles on the surface Apollo 15 green glass and trace-element distributions among Apollo 15 soils. *Proc. 7th Lunar Sci. Conf.*, 1701–1727.

COMPSTON W., FOSTER J. J., and GRAY C. M. (1975) Rb-Sr ages of clasts from within Boulder 1, Station 2, Apollo 17. *The Moon* **14**, 445–462.

CROWE B. M., FINNEGAN D. L., ZOLLER W. H., and BOYNTON W. V. (1987) Trace element geochemistry of volcanic gases and particles from 1983–1984 eruptive episodes of Kilauea Volcano. *J. Geophys. Res.* **92**, 13, 708–713, 714.

DePAOLO D. J. and WASSERBURG G. J. (1976) Nd isotopic variations and petrogenetic models. *Geophys. Res. Lett.* **3**, 249–252.

DICKINSON T., TAYLOR G. J., KEIL K., and BILD R. W. (1989) Germanium abundances in lunar basalts: Evidence of mantle metasomatism? *Proc. 19th Lunar Planet. Sci. Conf.*, 189–198.

DYMEK R. F., ALBEE A. L., and CHODOS A. A. (1975) Comparative mineralogy and petrology of Apollo 17 mare basalts: Samples 70215, 71055, 74255, and 75055. *Proc. 3rd Lunar Sci. Conf.*, 49–77.

EVENSEN N. M., MURTHY V. R., and COSCIO M. R., JR. (1973) Rb-Sr ages of some mare basalts and the isotopic and trace element systematics in lunar fines. *Proc. 4th Lunar Sci. Conf.*, 1707–1724.

GREEN D. H., RINGWOOD A. E., HIBBERSON W. O., and WARE N. G. (1975) Experimental petrology of Apollo 17 mare basalts. *Proc. 6th Lunar Sci. Conf.*, 871–893.

HALLIDAY A. N., MAHOOD G. A., HOLDEN P., METZ J. M., DEMPSTER T. J., and DAVIDSON J. P. (1989) Evidence for long residence times of rhyolitic magma in the Long Valley magmatic system: the isotopic record in precaldera lavas of Glass Mountain. *Earth Planet. Sci. Lett.* **94**, 274–290.

HORN P., JESSBERGER E. K., KIRSTEN T., and RICHTER H. (1975) ^{39}Ar-^{40}Ar dating of lunar rocks: Effects of grain size neutron irradiation. *Proc. 6th Lunar Sci. Conf.*, 1563–1591.

HUGHES S. S., DELANO J. W., and SCHMITT R. A. (1989) Petrogenetic modeling of 74220 high-Ti orange volcanic glasses and the Apollo 11 and 17 high-Ti mare basalts. *Proc. 19th Lunar Planet. Sci. Conf.*, 175–188.

HUNEKE J. C., JESSBERGER E. K., PODOSEK F. A., and WASSERBURG G. J. (1973) ^{39}Ar/^{40}Ar measurements in Apollo 16 and 17 samples and the chronology of metamorphic and volcanic activity in the Taurus-Littrow region. *Proc. 4th Lunar Sci. Conf.*, 1725–1756.

KESSON S. E. (1975) Mare basalts: Melting experiments and petrogenetic interpretations. *Proc. 6th Lunar Sci. Conf.*, 921–944.

KIRSTEN T. and HORN P. (1974) Chronology of Taurus-Littrow region—III: Ages of mare basalts and highland breccias and some remarks about the interpretation of lunar highland rock ages. *Proc. 5th Lunar Sci. Conf.*, 1451–1475.

KIRSTEN T., HORN P., and HEYMANN D. (1973) Chronology of Taurus-Littrow region I: Ages of two major rock types from the Apollo 17 site. *Earth Planet. Sci. Lett.* **20**, 125–130.

LONGI J., WALKER D., GROVE T. L., STOLPER E. M., and HAYS J. F. (1974) The petrology of Apollo 17 mare basalts. *Proc. 5th Lunar Sci. Conf.*, 447–469.

LUDWIG K. R. (1990) ISOPLOT: A plotting and regression program for radiogenic-isotope data, for IBM-PC compatible computers, version 2.01. *USGS Open-file Rept. 88-557.*

LUGMAIR G. W., SCHEININ N. B., and MARTI K. (1975) Sm-Nd age and history of Apollo 17 basalt 75075: Evidence for early differentiation of the lunar exterior. *Proc. 6th Lunar Sci. Conf.*, 1419–1429.

MEYER C., JR., McKAY D. S., ANDERSON D. H., and BUTLER P., JR. (1975) The source of sublimates on the Apollo 15 green and Apollo 17 orange glass samples. *Proc. 6th Lunar Sci. Conf.*, 1673–1699.

MINSTER J.-F., BIRCK F.-L., and ALLÈGRE C. J. (1982) Absolute age of formation of chondrites studied by the ^{87}Rb-^{86}Sr method. *Nature* **300**, 414–418.

MURALI A. V., MA M.-S., SCHMITT R. A., WARNER R. D., KEIL K., and TAYLOR G. J. (1977) Chemistry of 30 Apollo 17 rake basalts; 71597 a product of partial olivine accumulation (abstr.). *Lunar Sci.* **VIII**, 703–705.

MURTHY V. R. and COSCIO M. R., JR. (1976) Rb-Sr ages and isotopic systematics of some Serenitatis mare basalts. *Proc. 7th Lunar Sci. Conf.*, 1529–1544.

NEAL C. R. and TAYLOR L. A. (1989) Metasomatic products of the lunar magma ocean: The role of KREEP dissemination. *Geochim. Cosmochim. Acta* **53**, 529–541.

NEAL C. R., TAYLOR L. A., HUGHES S. S., and SCHMITT R. A. (1989) Apollo 17 high-Ti basalt petrogenesis: An integrated approach using whole-rock major and trace element analyses (abstr.). *Lunar Planet. Sci.* **XX**, 776–777.

NEAL C. R., TAYLOR L. A., PATCHEN A. D., HUGHES S. S., and SCHMITT R. A. (1990a) The significance of fractional crystallization in the petrogenesis of Apollo 17 Type A and B high-Ti basalts. *Geochim. Cosmochim. Acta* **54**, 1817–1833.

NEAL C. R., PACES J. B., TAYLOR L. A., HUGHES S. S., and SCHMITT R. A. (1990b) Two new Type C basalts: Petrogenetic implications for source evolution and magma genesis at the Apollo 17 site. *Lunar Planet. Sci.* **XXI**, 855–856.

NYQUIST L. E., BANSAL B. M., WIESMANN H., and JAHN B.-M. (1974) Taurus-Littrow chronology: Some constraints on early lunar crustal development. *Proc. 5th Lunar Sci. Conf.*, 1515–1539.

NYQUIST L. E., BANSAL B. M., and WIESMANN H. (1975) Rb-Sr ages and initial ^{87}Sr/^{86}Sr for Apollo 17 basalts and KREEP basalt 15386. *Proc. 6th Lunar Sci. Conf.*, 1445–1465.

NYQUIST L. E., BANSAL B. M., and WIESMANN H. (1976) Sr isotopic constraints on the petrogenesis of Apollo 17 mare basalts. *Proc. 7th Lunar Sci. Conf.*, 1507–1528.

NYQUIST L. E., BANSAL B. M., WOODEN J. L., and WIESMANN H. (1977) The Sr-isotopic constraints on the petrogenesis of Apollo 12 mare basalts. *Proc. 8th Lunar Sci. Conf.*, 1385–1415.

NYQUIST L. E., SHIH C.-Y., WOODEN J. L., BANSAL B. M., and WIESMANN H. (1979) The Sr and Nd isotopic record of Apollo 12 basalts: Implications for lunar geochemical evolution. *Proc. 10th Lunar Planet. Sci. Conf.*, 77–114.

NYQUIST L. E., REIMOLD W. U., BOGARD D. D., WOODEN J. L., BANSAL B. M., WIESMANN H., and SHIH C.-Y. (1981) A comparative Rb-Sr, Sm-Nd, and K-Ar study of shocked norite 78236: Evidence of slow cooling in the lunar crust? *Proc. 12th Lunar Planet. Sci. Conf. B*, 67–97.

NYQUIST L. E., BANSAL B. M., SHIH C.-Y., WIESMANN H., WOODEN J. L., and TAKEDA H. (1986) Rb-Sr and Sm-Nd internal isochron ages of a subophitic basalt clast from the Y75011 eucrite. *J. Geophys. Res.* **91**, B8, 8137–8150.

PAPIKE J. J., BENCE A. E., and LINDSLEY D. H. (1974) Mare basalts from the Taurus-Littrow region of the Moon. *Proc. 5th Lunar Sci. Conf.*, 471–504.

PAPIKE J. J., HODGES F. N., BENCE A. E., CAMEROON M., and RHODES J. M. (1976) Mare basalts: Crystal chemistry, mineralogy, and petrology. *Rev. Geophys. Space Phys.* **14**, 475–540.

PHILPOTTS J. A. and SCHNETZLER C. C. (1970) Apollo 11 lunar samples: K, Rb, Sr, Ba and rare-earth concentrations in some rocks and separated phases. *Proc. Apollo 11 Lunar Sci. Conf.*, 1471–1486.

RHODES J. M., HUBBARD N. J., WIESMANN H., RODGERS K. V., BRANNON J. C., and BANSAL B. M. (1976) Chemistry, classification, and petrogenesis of Apollo 17 mare basalts. *Proc. 7th Lunar Sci. Conf.*, 1467–1489.

RUTHERFORD M. J., HESS P. C., RYERSON F. J., CAMPBELL H. W., and DICK P. A. (1976) The chemistry, origin and petrogenetic implications of lunar granite and monzonite. *Proc. 7th Lunar Sci. Conf.*, 1723–1740.

RYDER G. (1990) A distinct variant of high-titanium mare basalt from the Van Serg core, Apollo 17 landing site. *Meteoritics* **25**, 249–258.

SALPAS P. A., TAYLOR L. A., and LINDSROM M. M. (1987) Apollo 17 KREEPy basalts: Evidence for Nonuniformity of KREEP. *Proc. 17th Lunar Planet. Sci. Conf.; J. Geophys. Res.* **92**, B4, E340–E348.

SCHAEFFER G. A. and SCHAEFFER O. A. (1977) ^{39}Ar-^{40}Ar ages of lunar rocks. *Proc. 8th Lunar Sci. Conf.*, 2253–2300.

SHIH C.-Y., HASKIN L. A., WIESMANN H., BANSAL B. M., and BRANNON J. C. (1975) On the origin of high-Ti mare basalts. *Proc. 6th Lunar Sci. Conf.*, 1255–1285.

SHIH C.-Y., NYQUIST L. E., BOGARD D. D., WOODEN J. L., BANSAL B. M., and WIESMANN H. (1985) Chronology and petrogenesis of a 1.8 g lunar granite clast: 14321,1062. *Geochim. Cosmochim. Acta* **49**, 411–426.

SHIH C.-Y., NYQUIST L. E., BOGARD D. D., BANSAL B. M., WIESMANN H., JOHNSON P., SHERVAIS J. W., and TAYLOR L. A. (1986) Geochronology and petrogenesis of Apollo 14 very high Potassium mare basalts. *Proc. 16th Lunar Planet. Sci. Conf.; J. Geophys. Res.*, **91**, B4, D214–D228.

SHIH C.-Y., BANSAL B. M., and WIESMANN H. (1990) Rb-Sr and Sm-Nd isotopic studies of an Apollo 17 KREEPy basalt (abstr.). *Lunar Planet. Sci.* **XXI**, 1148–1149.

STEIGER R. H. and JÄEGER E. (1977) Subcommission on geochronology: Convention on the use of decay constants in geo- and cosmochronology. *Earth Planet. Sci. Lett.* **36**, 359–362.

STETTLER A., EBERHARDT P., GEISS J., GRÖGLER N., and MAURER P. (1973) ^{39}Ar-^{40}Ar ages and ^{37}Ar-^{38}Ar exposure ages of lunar rocks. *Proc. 4th Lunar Sci. Conf.*, 1865–1888.

SYMONDS R. B. and REED M. H. (1991) Calculation of multicomponent chemical equilibria in gaseous-solid-liquid systems, Part II: Thermochemical data and applications to studies of high-temperature volcanic gases with examples from Mount St. Helens. *Amer. J. Sci.* (in press.).

SYMONDS R. B., ROSE W. I., REED M. H., LICHTE F. E., and FINNEGAN D. L. (1987) Volatilization, transport and sublimation of metallic and non-metallic elements in high temperature gases at Merapi Volcano, Indonesia. *Geochim. Cosmochim. Acta* **51**, 2083–2101.

TAYLOR G. J., WARNER R. E., KEIL K., MA M.-S., and SCHMITT R. A. (1980) Silicate liquid immiscibility, evolved lunar rocks and the formation of KREEP. In *Proc. Conf. Lunar Highlands Crust* (eds. J. J. PAPIKE and R. B. MERRILL), pp. 339–352. Pergamon Press.

TAYLOR S. R. (1982) *Planetary Science: A Lunar Perspective.* Houston: Lunar Planet. Inst.

TERA F., PAPANASTASSIOU D. A., and WASSERBURG G. J. (1973) A lunar cataclysm at −3.95 AE and the structure of the lunar crust. *Lunar Science IV,* 723-725. Lunar Institute, Houston.

TERA F., PAPANASTASSIOU D. A., and WASSERBURG G. J. (1974) Isotopic evidence for a terminal lunar cataclysm. *Earth Planet. Sci. Lett.* **22,** 1-21.

TITTERINGTON D. M. and HALLIDAY A. N. (1979) On the fitting of parallel isochrons and the method of maximum likelihood. *Chem. Geol.* **26,** 183-195.

TURNER G. and CADOGEN P. H. (1975) The history of lunar bombardment inferred from 40Ar-39Ar dating of highland rocks. *Proc. 6th Lunar Sci. Conf.,* 1509-1538.

TURNER G., CADOGAN P. H., and YONGE C. J. (1973) Argon selenochronology. *Proc. 4th Lunar Sci. Conf.,* 1889-1914.

UNRUH D. M., STILLE P., PATCHETT P. J., and TATSUMOTO M. (1984) Lu-Hf and Sm-Nd evolution in lunar mare basalts. *Proc. 14th Lunar Planet. Sci. Conf.; J. Geophys. Res.* **89,** B459-B477.

WARNER R. D., KEIL K., PRINZ M., LAUL J. C., MURALI A. V., and SCHMITT R. A. (1975) Mineralogy, petrology and chemistry of mare basalts from Apollo 17 rake samples. *Proc. 6th Lunar Sci. Conf.,* 193-220.

WARNER R. D., TAYLOR G. J., CONRAD G. H., NORTHROP H. R., BARKER S., KEIL K., MA M.-S., and SCHMITT R. A. (1979) Apollo 17 high-Ti mare basalts: New bulk compositional data, magma types and petrogenesis. *Proc. 10th Lunar Planet. Sci. Conf.,* 225-247.

WARREN P. H. (1985) The magma ocean concept and lunar evolution. *Ann. Rev. Earth Planet. Sci.* **13,** 201-240.

WARREN P. H., TAYLOR G. J., KEIL K., SHIRLEY D. N., and WASSON J. T. (1983) Petrology and chemistry of two "large" granite clasts from the Moon. *Earth Planet. Sci. Lett.* **64,** 175-185.

YORK D. (1969) Least-squares fitting of a straight line with correlated errors. *Earth Planet. Sci. Lett.* **5,** 320-324.

ZOLLER W. H., PARRINGTON J. R., and PHELAN KOTRA J. M. (1983) Iridium enrichment in airborne particles from Kilauea Volcano: January 1983. *Science* **222,** 1118-1121.